Susanne Dyrbøl

Heat transfer in Rockwool modelling and method of measurement

Part II:

Modelling radiative heat transfer in fibrous materials

Technical University of Denmark
Department of Buildings and Energy

Rockwool International A/S and Rockwool A/S

The Danish Academy of Technical Science EF-568

Ph.D. – thesis, May 1998

Technical University of Denmark, Department of Buildings and Energy
Rockwool International A/S and Rockwool A/S
The Danish Academy of Technical Science EF-568

Heat transfer in Rockwool modelling and method of measurement

Part II: Modelling radiative heat transfer in fibrous materials

Ph.D. – thesis, May 1998 by Susanne Dyrbøl

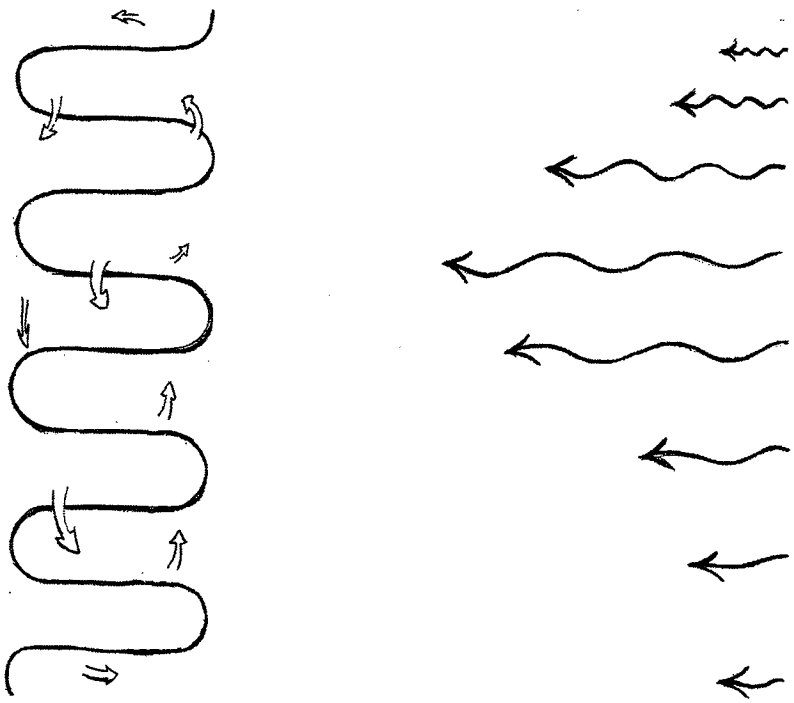

Preface

The Danish Academy of Technical Science, together with Rockwool International A/S and Rockwool A/S, have financed this project, the aim being to support research in the field of building physics in Denmark.

The work was carried out at the Department of Buildings and Energy at the Technical University of Denmark under the supervision of Professor Svend Svendsen and Professor Arne Elmroth from Lund Technical University to whom I owe a great debt of thanks for sharing their views and for helping me during the project.

The analysis of radiative heat transfer models has been carried out in collaboration with Associate Professor Flemming Andersen, Aalborg University. His great engagement and support have been invaluable throughout the entire project.

Special thanks are due to Professor Carl-Erik Hagentoft for sharing his computer code for calculating convection in porous media and for valuable discussions during the project, and to Professor Timothy W. Tong for sharing his computer code for calculating the radiative efficiencies of fibres.

The method of estimating the fibre orientation in fibrous materials has been developed in collaboration with M.Sc. Torben Mandrup Jacobsen, Rockwool International A/S, and with assistance from the Dept. of Mathematical Modelling, Technical University of Denmark.

I extend my sincere gratitude to the many people who have been involved in the project in various ways. Especially to my supervisors Section Leader Erik Rasmussen and Senior Engineer Helge Høyer at Rockwool International A/S, for many valuable discussions, to the laboratory staff at both the University and at Rockwool who provided help with the measurements, to my colleague Jørgen Schultz for assistance with data recording and for many valuable hours and discussions together with Lise Boye-Hansen, Kirsten Engelund Thomsen and Finn Kristiansen over the past three years, to Gitte Nellemose for making the drawings in the report and to Solvej Allen, Gyda Metz and Maj Britt Højgaard for linguistic help.

Copenhagen, May 1998

Susanne Dyrbøl

Part II Modelling radiative heat transfer in fibrous materials

Contents

Preface
Summary i
Resumé (in Danish) vi

Nomenclature xi

1. Introduction 1
1.1 Background 1
1.2 Purpose and limitations of the study in part II 3
1.3 Structure of the thesis 4
1.3.1 Structure of part II 4

2. Studies of literature 6
2.1 General theory and approximating methods 6
2.2 Calculation of radiative properties in fibrous materials 6
2.3 Previous analysis on fibre glass 8

3. Modelling radiative heat transfer in fibrous materials 9
3.1 Physical description of problem 9
3.2 Mathematical model – general heat transfer equations 10
3.2.1 The two flux-model 13
3.2.2 Spherical harmonics method (P-N method) 15

4. Theoretical determination of radiative properties in fibre materials 17
4.1 Introduction 17
4.2 Approximating wavelength dependence on optical properties 18
4.3 Calculation of scattering and absorption coefficients in fibrous materials 19
4.4 Mean coefficients 23

5. Determination of texture in fibrous materials 24
5.1 Introduction 24
5.2 Method 24
5.2.1 Images 25
5.2.2 Determination of dominant orientation 27
5.2.3 Determination of orientation distribution – von Mises 28
5.3 Example of orientation distributions measured on fibrous materials 29
5.4 Summary 32

6. Conclusion 33
6.1 Recommendations for future work 34
62. Commercial perspective 34

Biography 36

Appendix A: Comparison of Radiative Heat Transfer Models in Mineral Wool at Room Temperature. Conference paper. 39

Appendix B: Modelling Radiative Heat Transfer in Fibrous Materials: the use of Planck Mean Properties compared to Spectral and Flux-weighted Properties. Article accepted for publication in JQSRT 53

Appendix C: Orientation estimation 66

Summary

Preconditions

Fibrous materials are some of the most widely used materials for thermal insulation. In this project the focus of interest has been on fibrous materials for building application. Interest in improving the thermal properties of insulation materials is increasing as legislation is being tightened to reduce the overall energy consumption. A knowledge of the individual heat transfer mechanisms – whereby heat is transferred within a particular material is an essential tool to improve continuously the thermal properties of the material.

Heat is transferred in fibrous materials by four different transfer mechanisms: conduction through air, conduction through fibres, thermal radiation and convection. In a particular temperature range the conduction through air can be regarded as a constant, and conduction through fibres is an insignificant part of the total heat transfer. Radiation, however, constitutes 25-40% of the total heat transfer in light fibrous materials. In Denmark and a number of other countries convection in fibrous materials is considered as non-existent when calculating heat transmission as well as when designing building structures.

Two heat transfer mechanisms have been the focus of the current project: radiation heat transfer and convection.

The radiation analysis serves to develop a model that can be used in further work to gain a wider knowledge of the way in which the morphology of the fibrous material, i.e. fibre diameter distribution, fibre orientation distribution etc., influences the radiation heat transfer under different conditions.

The convection investigation serves to examine whether considering convection as non-existent is a fair assumption to use in present and future building structures. The assumption applied in practically is that convection makes a notable difference only in very thick insulation, at external temperatures below -20°C, and at very low densities. For large thickness dimensions the resulting heat transfer through the fibrous material will be relatively small, which means that a relatively small increase in heat loss by convection may counterbalance part of the savings achieved by increasing the thickness.

Heat radiation analysis – method - delimitation

A literature study has been carried out, primarily in regard to the theoretical modelling of radiation heat transfer in fibrous materials. This study has led to the overall conclusion that there are two important aspects within thermal radiation.

- One aspect is the radiation heat transfer itself, in which the mathematical model describing the radiation heat transfer in fibrous materials cannot be solved analytically. In the literature there are several different approximation methods for solving the radiative transport equation, the two-flux method being that most commonly used for fibrous materials, due to its simplicity. It has not been possible to assess the significance of the simplification for the calculated radiation heat transfer within the temperature range relevant to building insulation.

- The other aspect is the determination of the radiative properties of the fibrous material which are part of the radiation transport equation. In the literature these are used partly on a spectral basis, and partly as weighted values with a consequent high degree of simplification of the equation systems to be solved. Neither in this case has it been possible to find an assessment of the significance of using weighted values rather than spectral values when calculating radiation heat transfer in the specific temperature range. The radiative properties depend on the morphology of the fibrous material, the only parameter that cannot be determined experimentally being the fibre orientation distribution.

There are many aspects to the field "radiation transfer in fibrous materials", and it has therefore been necessary to limit the extent of the project. The delimitation has been based on the considerations identified from the literature survey and the shortness of time allocated to the project.

The radiation analysis has been delimited to include:

- a theoretical examination of the precision achieved when applying the two-flux model as an approximation for the radiative transport equation, compared with the spherical harmonics method, which has proved to give high precision in earlier cases of radiation problems with an analytical solution; in order to simplify the equation systems when comparing the two approximation methods, the Planck-weighted radiative properties have been used in the radiation transport equation;

- a theoretical examination of the precision achieved when applying the Planck-weighted radiative properties as opposed to a spectral solution when the two-flux model is used for approximating the radiation transport equation;

- developing a method that can be used to determine an estimate of the fibre orientation distribution.

The concepts of thermal radiation introduced in this project can well be applied to other thermal radiation problems arising when the radiative properties of the material depend on the wavelength of the radiation. In the present project the focus has been on fibrous materials for building insulation, which has determined the geometry and the conditions applied in the investigations, i.e. steady-state one-dimensional heat flow at a mean temperature of 10°C.

Heat radiation analysis – main results

A computer model for the heat transfer in fibrous materials has been developed. The model includes conduction in air and fibres, heat exchange between the two phases, and radiative heat transfer. As an approximation to the radiation transport equation, the two-flux model and the spherical harmonics method with an arbitrary high approximation order have been applied. In the computer code using the two-flux model a spectral solution of the radiation transport equation can be obtained.

Comparison of the two approximation methods shows that:

- the two-flux model underpredicts the radiative heat flux by approximately 15%, whereas the spherical harmonics method is more exact;
- considering only the computed total radiative heat flux, the same result is achieved with the simplest spherical harmonics method (P-1) as with a higher approximation order;
- the air and the fibre temperature are the same at the applied temperature level.

Comparison of the radiative heat flux obtained using the Planck-weighted radiative properties as opposed to the spectral solution led to the following conclusions:

- using the Planck-weighted properties underpredicts the radiative heat flux in the centre of the fibrous materials by approximately 15% compared to the spectral solution;
- it is not possible to determine a suitable weighting function for the radiation constants without first knowing the spectral solution.

The radiation properties in fibrous materials are determined by the morphology of the material; hitherto it has not been possible to measure the distribution of fibre orientation in the material. In connection with the project, a method for characterising the macro texture in fibrous materials has been developed. The dominant direction in the macro texture is measured by means of image analysis performed on partial images of the texture. By assuming that the macro texture reflects the fibre structure within the material, an estimate of the fibre orientation distribution can be approximated on the basis of the distribution of the dominant directions measured on the macro texture.

Convection investigation – method - delimitation

Convection may be divided into two fields: natural convection and forced convection. The overall delimitation for this project is natural convection.

The literature on performed theoretical and experimental research concerning natural convection has been studied. The literature survey can be summarised as follows.

- The mathematical models describing convection can be approximated using a series of dimensionless numbers. Depending on the geometry of the structure, a critical limit value of the Rayleigh number, Ra_{cr}, exists for the point at which the convection starts to influence the total heat transfer in the material. This critical value is theoretically and experimentally well defined for horizontal structures, whereas for vertical structures it is empirically determined but not clearly defined in the literature. For fibrous materials the permeability and the heat conductivity are the main parameters determining the effect of convection.
- Most examinations have been concentrated on determining the influence on the total heat transfer in the material. Introducing permeable borders or insulation error into the material increases the influence of convection, which becomes obvious at an earlier stage.

In order to be able to assess the convection conditions when the material is placed in a real structure it is necessary to know the convection conditions in the material itself. To facilitate the experimental work, a convection apparatus with a measuring field of 3·1 m^2 was designed, within which it is possible to measure a specimen thickness ranging from 0.1 m – 0.5 m. The boundary conditions are achieved immediately in the apparatus design. To support the interpretation of the measurements, the experimental work has been supplemented with numerical calculations.

The project was limited to an experimental search for the occurrence of natural convection in fibrous materials of different permeability under the following conditions:

- "perfectly" installed materials
- impermeable and isothermal boundaries
- measuring of fibrous materials with dimensions similar to those applied in building structures.

The effect of building physics strain in connection with convection, such as comfort and moisture transfer, has not been examined in the project.

Convection investigation – main results

The contribution of natural convection to the total heat transfer has been experimentally examined for two fibrous materials of different permeability and heat conductivity. The measurements performed have been supported by numerical calculations.

Both the measurements and the concurrent computations show a clear convection-induced redistribution of the heat flow in the material in the form of an increased heat flow primarily through the lower part of the vertical structure, and a decreased heat flow primarily through the upper part.

- The redistribution of the convection-induced heat flow is distinct, even at a material thickness as low as 0.2 m and at a temperature gradient of 20°C across the material.

- In the low permeable material the redistribution of the heat flow has no influence on the total heat flow through the material.

- In the highly permeable material the convection caused an increase in the total heat flow through the material.

Establishing that convection occurs even in "perfectly" installed materials with low permeability, impermeable boundaries and at small temperature differences means that the assumption that convection is non-existent, which has been the basis of the common practice, is invalid even under the most ideal conditions.

The measuring principle of the convection apparatus in which a three-dimensional guard system is used was found suitable for measuring one-dimensional heat flows at thick specimen dimensions. The measuring properties of the convection apparatus were verified on an impermeable material at a thickness of 0.5 m, in which good agreement with laboratory measurements on 0.1 m thick samples was found.

When performance-testing the apparatus, problems were found in a few of the guard sections. The chosen solution to this problem proved to be less optimal during the measuring. How this problem may have influenced the measurements is analysed and discussed in the report.

Resumé

Forudsætninger

Fibermaterialer hører til blandt de dominerende materialer indenfor termisk isolering. I dette projekt er fokuseret på fibermaterialer til bygningsisolering, hvor interessen for at forbedre materialernes termiske egenskaber hele tiden øges i takt med, at lovgivningen skærpes for at reducere det totale energiforbrug. Her er kendskabet til de enkelte transportmekanismer, hvorved varme transporteres i materialet, et væsentligt og nødvendigt værktøj for fortsat at kunne forbedre materialets termiske egenskaber.

Varmetransporten i fibermaterialer foregår ved fire forskellige transportmekanismer: Ledning i luft, ledning i fibre, varmestråling samt konvektion. Ledning i luften kan indenfor det aktuelle temperaturområde betragtes som værende af en konstant størrelse, og ledning i fibrene udgør en forsvindende lille del af den samlede varmetransport. Varmestrålingen udgør derimod mellem 25 - 40% af den samlede varmetransport ved lette fibermaterialer. I Danmark og en lang række andre lande betragtes konvektion i fibermaterialer som et ikke-forekommende fænomen såvel i varmetabsberegninger som ved design af bygningskonstruktioner.

I det udførte projekt er der fokuseret på to af varmetransportmekanismerne: varmestråling og konvektion.

Varmestrålingsanalysen har som formål at udarbejde en model, der kan anvendes i det videre arbejde med at opnå et større kendskab til, hvordan fibermaterialets morfologi (fiber diameter fordeling, fiber orientering, etc.) påvirker strålingsvarmetransporten under forskellige betingelser.

Konvektionsundersøgelsen har til formål at undersøge eksperimentelt om den i praksis anvendte antagelse, at konvektion kun har nævneværdig betydning ved meget store isoleringstykkelser, udvendige temperaturer lavere end -20°C, samt ved meget lave densiteter, er en rimelig antagelse i forbindelse med nutidens og fremtidens byggeri. Ved store isoleringstykkelser vil den resulterende varmetransport gennem materialet være relativ lille, og derfor vil en relativ lille forøgelse i varmetabet på grund af konvektion kunne modsvare en del af den opnåede energibesparelse ved en forøget isoleringstykkelse.

Varmestrålingsanalyse - metodik – afgrænsning

Der er her udført et litteratur studie, primært indenfor teoretisk arbejde med at modellere strålingsvarmetransport i fibermaterialer. Studiet har ført til den overordnede konklusion, at der er to vigtige aspekter inden for termisk stråling i forbindelse med fibermaterialer.

- Det ene aspekt er selve strålingsvarmetransporten, hvor den matematiske model, der beskriver strålingsvarmetransporten i fibermaterialer, ikke kan løses analytisk men ved flere forskellige approksimative løsningsmetoder, hvor two-flux metoden på grund af sin enkelhed er den hyppigst anvendte approksimation ved fibermaterialer. Det har ikke været muligt, at finde en vurdering af hvad forenklingen betyder for den beregnede varmestråling indenfor det temperaturområde, der er aktuelt for bygningsisolering.

- Det andet aspekt er bestemmelse af fibermaterialets strålingsegenskaber, der indgår i strålingstransportligningen. I litteraturen anvendes disse dels på spektral basis og dels som vægtede værdier med en deraf følgende stor forenklingsgrad af de ligningssystemer, der skal løses. Det har ikke været muligt at finde en vurdering af, hvilken betydning anvendelsen af vægtede værdier frem for spektrale værdier har for den beregnede varmestråling i det aktuelle temperaturområde og for fibermaterialets morfologi. Strålingsegenskaberne afhænger af fibermaterialets morfologi, hvor den eneste parameter, der ikke kan bestemmes eksperimentelt, er fiberorienteringen.

Der er mange aspekter indenfor emnet "varmestråling i fibermaterialer", og det har derfor været nødvendigt at afgrænse udstrækningen af opgaven. Den valgte afgrænsning er foretaget med udgangspunkt i problemstillingen fra litteraturstudiet samt den begrænsede projekttid.

Varmestrålingsanalysen er afgrænset til at omfatte:

- en teoretisk undersøgelse af den opnåede nøjagtighed ved at anvende two-flux modellen som approksimation til strålingstransportligningen sammenlignet med spherical harmonics metode der ved stålingsproblemer med en analytisk løsning tidligere har vist at give en høj præcision. For at simplificere ligningssystemerne ved sammenligningen af de to approksimationsmetoder er Planck-vægtede strålingskoefficienter anvendt ved sammenligningen

- en teoretisk undersøgelse af den opnåede nøjagtighed ved at anvende Planck-vægtede strålingskoefficienter i forhold til en spektral løsning. Two-flux modellen er her anvendt som approksimation til strålingstransportligningen

- udvikling af en metode, der kan anvendes til at estimere en fiber-orienteringsfordeling.

De udførte betragtninger i projektet vedrørende varmestråling kan umiddelbart overføres på mange andre termiske strålingsproblemer, hvor materialets strålingsegenskaber afhænger af strålingens bølgelængde. I det udførte projekt er der fokuseret på fibermaterialer til bygningsisolering, hvilket har bestemt geometrien og forholdene, der er anvendt i de udførte undersøgelser; en-dimesional stationær varmestrøm ved en middeltemperatur på 10°C.

Varmestrålingsanalyse - hovedresultater

Der er udviklet en computermodel til beregning af varmetransporten i fibermaterialer. Modellen inkluderer ledning i luft og fibre, varmeoverføring mellem luft og fibre, samt termisk strålingstransport. Som approksimation til strålingstransportligningen er anvendt two-flux modellen og spherical harmonics metoden med en vilkårlig høj approksimationsorden. I computermodellen, hvor two-flux modellen anvendes, kan der bestemmes en spektral løsning af strålingstransportligningen.

Den udførte sammenligning af de to approksimationsmetoder viser at:

- Two-flux modellen underbestemmer strålingseffekten med ca. 15% sammenlignet med den mere præcise spherical harmonics metode
- betragtes kun den beregnede resulterende strålingseffekt, opnås samme resultat med den mest simple spherical harmonics metode (P-1) som ved anvendelse af en højere approksimationsorden
- luft og fibre har samme temperatur ved det anvendte temperaturniveau.

Sammenligningen af strålingseffekten beregnet med Planck-vægtede strålingskonstanter i forhold til den spektrale løsning førte til følgende konklusioner:

- anvendelsen af Planck-vægtede strålingskonstanter giver en strålingseffekt, der er ca. 15% lavere i forhold til den spektrale løsning i fiber materialer
- det er ikke muligt at bestemme en passende vægtningsfunktion for strålingskonstanterne uden først at kende den spektrale løsning.

Strålingskonstanterne i fibermaterialer bestemmes af materialets morfologi, hvor vi hidtil ikke har været i stand til at måle fordelingen af fiberorienteringer i materialet. Der er i forbindelse med projektet udviklet en metode til karakterisering af makrostrukturen i fibermaterialer. Den foretrukne retning i makrostrukturen måles ved hjælp af billedanalyse udført på delbilleder af strukturen. Ved at antage, at makrostrukturen afspejler materialets fiberstruktur, kan et estimat for fiberorienteringsfordelingen approksimeres med fordelingen af de fremtrædende retninger i makrostrukturen.

Konvektionsundersøgelse - metodik - afgrænsning

Konvektion inddeles i to områder: Naturlig konvektion og tvungen konvektion. Dette projekt er overordnet afgrænset til kun at omfatte naturlig konvektion.

Der er udført et litteraturstudie over udført teoretisk og eksperimentelt arbejde indenfor naturlig konvektion. Litteraturstudiet kan summarisk sammenfattes i nedenstående.

- De matematiske modeller, der beskriver konvektion, kan approksimeres med en række dimensionsløse tal. Afhængig af konstruktionens geometri eksisterer der en kritisk grænseværdi for Rayleigh tallet Ra_{cr}, for hvornår konvektionen påvirker varmetransporten i materialet. Den kritiske værdi er både teoretisk og eksperimentelt veldefineret for horisontale konstruktioner, hvorimod den for vertikale konstruktioner er empirisk fastlagt og ikke helt entydigt bestemt i litteraturen. For fibermaterialer er permeabiliteten og varmeledningsevnen de væsentligste parametre for effekten af konvektion.
- De fleste undersøgelser er koncentreret om at bestemme den resulterende effekt på varmetransporten i materialet. Ved at introducere permeable grænser eller isoleringsfejl i materialet øges effekten af konvektion og konvektionen bliver tydelig på et tidligere tidspunkt.

For at være i stand til at vurdere konvektionsforholdene når materialet anbringes i en virkelig konstruktion er det nødvendigt også at kende konvektionsforholdene i selve materialet. Til det eksperimentelle arbejde er opbygget et konvektionsapparat med et målefelt på 3·1 m^2, hvor det er muligt at måle materialetykkelser i intervallet 0.1 m - 0.5 m. Grænsebetingelserne er tilnærmet gennem apparatdesignet. Som hjælp til fortolkningen af de udførte målinger er det eksperimentelle arbejde understøttet af numeriske beregninger.

Projektet er afgrænset til eksperimentelt at undersøge forekomsten af naturlig konvektion i fibermaterialer med forskellig permeabilitet under følgende betingelser:

- "perfekt" installerede materialer
- impermeable og isoterme grænser
- måling på materialet i samme dimensioner som det forekommer indenfor bygningsisolering.

Effekten af bygningsfysiske belastninger i forbindelse med konvektion herunder komfort og fugt transport er ikke undersøgt.

Konvektionsundersøgelse - hovedresultater

Betydningen af naturlig konvektion for det totale varmetab er eksperimentalt undersøgt for to fibermaterialer med forskellig permeabilitet og varmeledningsevne. De udførte målinger er understøttet af numeriske beregninger.

Både målinger og de tilhørende beregninger viser en tydelig omfordeling af materialets varmetab på grund af konvektion i form af et forøget varmetab primært gennem den nederste del i den vertikale konstruktion og en reduktion af varmetabet primært gennem den øverste del i konstruktionen.

- Omfordelingen af materialets varmetab på grund af konvektion ses tydeligt, selv ved en materiale tykkelse på 0.2 m og helt ned til en temperaturgradient over materialet på 20°C.

- Ved materialet med lav permeabilitet påvirker omfordelingen af varmetabet i materialet ikke det totale varmetab.

- Ved materialet med høj permeabilitet medførte konvektionen at det totale varmetab gennem materialet blev forøget.

Konstateringen af, at der forekommer konvektion selv i "perfekt" installerede materialer med lav permeabilitet, impermeable grænser og ved selv små temperaturforskelle betyder, at forudsætningen for den hidtil anvendte praksis, hvor konvektion negligeres ikke er tilstede selv under de mest ideelle betingelser.

Måleprincippet i konvektionsapparatet, hvor der anvendes et tre-dimensionelt guardsystem, er fundet velegnet til måling af en-dimensionale varmestrømme ved store isoleringstykkelser. Konvektionsapparatets måleegenskaber er verificeret på et impermeabelt materiale, hvor der ved en prøvetykkelse på 0.5 m blev fundet fin overensstemmelse med laboratoriemålinger udført på prøvetykkelser af 0.1m.

Ved apparattesten blev der konstateret problemer med enkelte guardsektioner. Den valgte løsning på problemet har i målingerne vist sig at kunne forbedres. Hvorledes de udførte målinger er påvirket af dette er analyseret og kommenteret i rapporten.

Nomenclature

Latin letters

a_v	surface area of fibres per m³ fibre material [m^{-1}]
b	backscatter factor
D	fibre diameter [m]
e_b	blackbody emissive power [W/m^2], total or [W/m^3] spectral
f_m	factor in expression of the phase function
f_v	particle volume fraction ($\rho_{fibre}/\rho_{solid}$) [-]
h	heat transfer coefficient [$W/m^2 \cdot K$]
i	total intensity [$W/m^2 \cdot sr$], total or [W/m^3] spectral
k	index of absorption
l_f	length of a fibre
l_x, l_y, l_z	unit vectors in x, y, z coordinate directions
L	thickness of the fibre layer [m]
n	index of refraction
N	order of spherical harmonics approximation
N_{tot}	number of particles per unit volume
$P_m(\mu)$	Legendre polynomials [m]
q	heat flow rate [W/m^2], total or [W/m^3] spectral
Q_a	absorption efficiency [-]
Q_s	scattering efficiency [-]
$\underline{r}$	position vector
S	coordinate along path of radiation
T	temperature [K]
z	location [m]

Greek letters

α	angle between incident radiation and the directional normal of the fibre which is located in the plane formed of $\underline{r}_f$ and $\underline{r}_i$
β	azimuthal angle of fibre
φ	polar angle of fibre
ϕ	porosity
Φ	scattering phase function
θ	polar angle of radiation
Θ	angle between incident and scattered radiation
λ_g	thermal conductivity of gas [W/m·K]
λ_s	thermal conductivity of solid [W/m·K]
λ	wavelength [m]
∇	gradient
μ	direction cosine, $\mu = \cos\theta$
ρ	mass density [kg/m^3]
σ	Stefan-Boltzmann constant ($\sigma = 5.67051 \cdot 10^{-8}$ $W/m^2 \cdot K^4$)
σ_a	absorption coefficient [m^{-1}]
σ_s	scattering coefficient [m^{-1}]
ξ	azimuthal angle of radiation
$\Psi_m(z)$	function in the spherical harmonics [$W/m^2 \cdot sr$]
ω	solid angle

Subscript

a	absorption
b	blackbody
cd	conduction
cv	convection
f	fibre
g	gas
i	incident
λ	wavelength
Pl	Planck
r	radiation
s	solid or scattering
tot	total
x, y, z	direction coordinates
+/-	positive/ negative direction of z-axis

Superscript

r	radiation
‘	directional quantity

1. Introduction

1.1 Background

Fibrous material is one of the most frequently used materials for building insulation. The demands for the thermal performance of both the building as a whole as well as the individual building elements are currently intensified in order to reduce the overall heat loss. This project has therefore focused on the thermal performance of fibrous materials. To be able to improve the performance of these materials in the long term, it is important to know the influence of various parameters on the thermal performance.

Fibrous materials are heterogeneous and consist of two phases; a gas phase (air) and a solid matrix (fibres). In such a material, heat is transmitted in three physically different ways: by conduction in fibres and gas, by radiation, and by convection.

In heat conduction, the energy is transmitted through lattice vibration in the solid and by random collision of molecules in the gas.

Transfer of energy by radiation takes place through electromagnetic waves between the fibres while the air does not interact with radiation.

Natural convection is caused by temperature-induced density differences in the gas phase which generate an airflow in the material.

Assuming little or no interaction between the different heat transfer mechanisms, the total heat transfer across the fibrous material is described by eq. (1.1):

$$\bar{q}_{tot} = \bar{q}_{cd} + \bar{q}_{r} + \bar{q}_{cv} \tag{1.1}$$

from which the thermal conductivity of the fibrous material is obtained by using Fourier's law:

$$\bar{q}_{tot} = -\lambda_{tot} \cdot \nabla T \tag{1.2}$$

In practice, the effect of convection is usually disregarded, and a semi-empirical relation, where the apparent thermal conductivity is a function of the density of the fibrous material, can be expressed according to Bomberg and Klarsfeld [1983], eq.(1.3):

$$\lambda_{tot} = A + B \cdot \rho + \frac{C}{\rho} \tag{1.3}$$

in which the constant A is the air conduction term λ_{air}, $B \cdot \rho$ is the conduction in the fibres λ_{fibre}, and C/ρ is the radiative term λ_r. The constants B and C must be determined by measurements, and are related to the specific material while the air conduction term is a constant at constant temperatures $\lambda_{air,10°C} \sim 0.0249$ W/m·K (Pitts and Sissom, 1997). The solid conduction term is insignificant in low-density materials $\lambda_{fibre} \sim 0.001$-$0.002$W/mK, whereas the radiation part represents approximately 0.008-0.020 W/m·K at room temperature when dealing with low-density materials, e.g. in the interval 10-40 kg/m^3. These models are able to predict the apparent thermal conductivity when only the density is changed but they are not

detailed enough in many other cases. For example, when the distribution of fibre diameters or fibre orientations in the fibrous material is changed, eq. (1.3) cannot be used to predict the change in thermal conductivity.

Figure 1.1 shows an example of the contribution by conduction in air, in fibres, and by radiation to the total thermal conductivity in a typical fibrous material for building application, the convection part being disregarded.

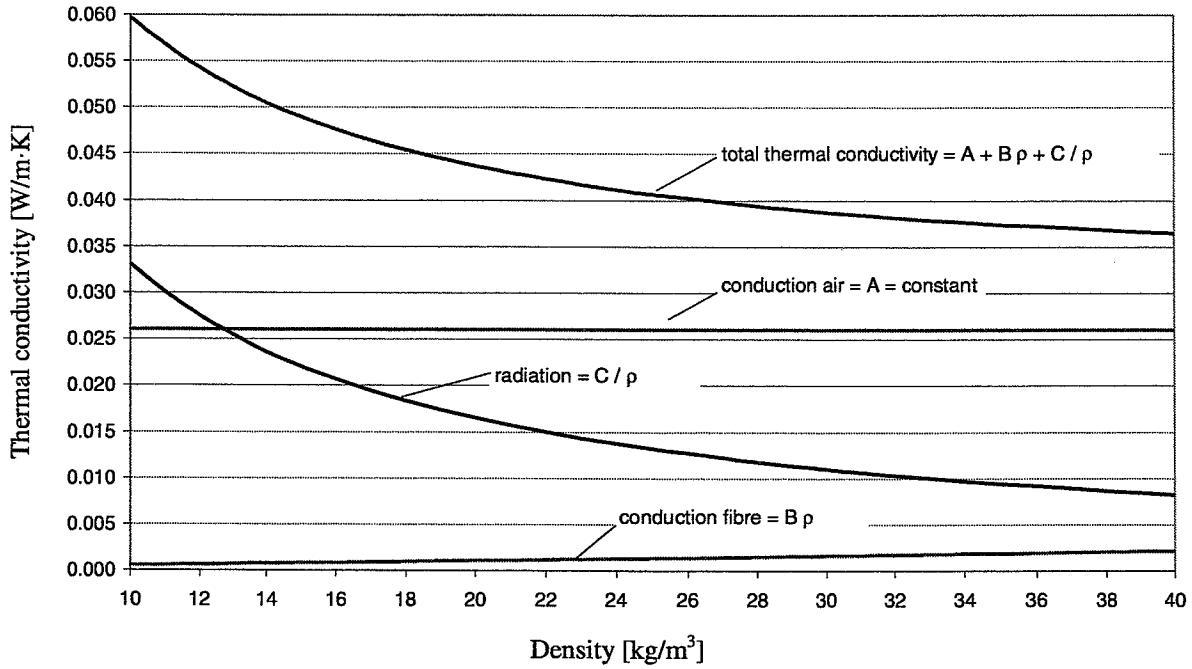

Figure 1.1: Contributions from conduction in air, conduction in fibres and radiation to the total thermal conductivity in a mineral fibre insulation for building application according to Kumaran [1996] in which the constants A = 0.02606 W/m·K, B = $5.48 \cdot 10^{-5}$ W·m²/K·kg and C = 0.331W·kg/K·m⁴ are used at a temperature of 10°C in eq. (1.3). However, minor variations in the constants will exist when comparing with the work of other authors.

The air conduction must be considered as a part of the total thermal conductivity which cannot be influenced unless the fibrous material is in vacuum or the air is replaced by an inert gas; the conduction due to the fibres is negligible when considering low-density materials. On this background, attention in the current project has been centred on two subjects:

- examining whether disregarding natural convection in fibrous materials is an acceptable assumption when dealing with thick dimensions (Part I)
- studying the modelling of radiative transfer in fibrous materials (Part II)

The present report (Part II) includes only studies of the modelling of radiative heat transfer in fibrous materials.

1.2 Purpose and limitations of the study in part II

The modelling of radiative transfer involves two parallel and equally important subjects:

- solve the radiative transport equation (R.T.E.) concerning the actual problem
- determine the radiative properties of the fibrous materials

Various approximative methods are available in the literature for solving the R.T.E. of which the most commonly used is the two-flux model, due to its simplicity.

Therefor, the first purpose of this work was:

- ***to investigate the applicability and the accuracy of the two-flux model in relation to fibrous materials for building application and to develop a computer code which can be used in future work***

This investigation is presented in appendix A.

The two-flux model is evaluated by comparison to the spherical harmonics method which is known to give good results when modelling radiative transfer in combustion systems (Selcuk, 1994). The computer model includes coupled radiation and conduction in one dimension, in which only steady-state conditions have been considered.

In order to simplify the problem, and not making a spectral analysis, the Planck-weighted radiative properties have been used in the computer model when investigating the applicability of the two-flux model.

In literature available on the subject of analysing the radiative heat transfer in fibrous material, either the Planck-weighted radiation coefficients are used in the R.T.E. (e.g. Tong et al. 1990) or a spectral analysis is performed of the R.T.E. (e.g. Langlais et al., 1995). From the performed literature survey there seems to be a lack of knowledge concerning the use of mean properties when modelling radiative heat transfer in fibrous materials.

Therefore, the second purpose of this work was:

- ***to investigate the accuracy of the radiative heat flux obtained using the Planck-weighted properties in the two-flux model, compared to the detailed spectral two-flux model, in case of fibrous materials***

This investigation is presented in appendix B.

The theory of calculating the radiative properties of a single, infinitely long cylinder is assumed to be known and has not been dealt with here.

When calculating the radiative properties of a cloud of fibres, the fibre diameter distribution, the fibre orientation distribution, and the optical properties of the fibres have to be taken into account. Unfortunately, we are not able to measure the fibre orientation distribution in the space whereas the diameter distribution, and the optical properties of the fibres can be measured.

Therefore, the third purpose of this work was:

- ***to develop an experimental procedure for determining an estimate of the fibre orientation distribution in fibrous materials***

As a result of the investigation, the possibility of measuring the orientation of the individual fibres has been evaluated as not possible due to the size and shape of the fibres which are not straight. Instead, the texture in the fibrous material is assumed to be able to characterise the orientation distribution of the individual fibres.

1.3 Structure of the thesis

The thesis consists of two separate reports which deal with the subjects:

- Part I: "Effect of natural convection on heat transfer in fibrous material"
- Part II: "Modelling radiative heat transfer in fibrous material"

The two reports can be read independently, and only the structure of part II will be presented in the following. The structure of part I is described in part I.

1.3.1 Structure of part II

The investigations of modelling radiative heat transfer in fibrous materials are presented in the conference paper and the article in appendix A and appendix B, respectively. The report contains mainly a brief summary presentation of the theory and limitations when modelling radiative heat transfer in fibrous materials.

Chapter 2 contains a brief review of previous work in the field of determining the radiative properties of fibrous materials and analysing the radiative heat transport in fibrous materials.

Chapter 3 presents the geometry of the fibrous materials considered together with the assumptions applied when modelling the radiative heat transfer. The mathematical model used in the computer code is presented together with a brief introduction of the two-flux model and the spherical harmonics methods which are used to solve the R.T.E.

Chapter 4 describes the calculation of radiative properties of a fibrous material. The calculation is presented on a spectral basis and as the Planck-weighted properties.

Chapter 5 describes the preliminary method developed to determine an estimate of the orientation distribution of the fibres. The dominating orientation in the texture in arbitrary small areas of the fibrous materials is determined by image analysis. The orientation distribution is approximated by a statistical distribution which observes that the measured angles all will be within 2π.

Chapter 6 contains the conclusion, which summarises the results presented in appendix A and B.

Appendix A contains the paper "Comparison of radiative heat transfer models in mineral wool at room temperature". In the paper, the radiative heat transfer in fibrous materials is compared when the two-flux model and the spherical harmonics method are used to solve the R.T.E.

Appendix B contains the article "Modelling radiative heat transfer in fibrous materials: the use of Planck-weighted properties compared to spectral and flux-weighted properties", in which the calculated radiative flux is investigated when using different weighting methods to calculate the weighted radiative properties in the two-flux model compared to the spectral solution.

The literature to which references have been made in this report is described in the bibliography whereas the literature to which references have been made in the appendices is described in the references, which form part of the appendices.

To the extent possible, symbols according to ISO and Siegel and Howell [1992] have been used. Any other symbols are explained in the text when used. SI units are used throughout the entire thesis.

2. Studies of literature

The modelling of radiative heat transfer in fibrous materials includes three phases:

- defining the equation system which describes the physical problem. The radiative transport equation (R.T.E.) will be part of this description. For fibrous material the R.T.E. can not be solved analytically.
- determining the radiative properties of the fibrous material which forms part of the R.T.E.
- choosing an appropriate approximation method to solve the R.T.E.

In the present modelling of radiative heat transfer in fibrous materials for various applications have been studied by many authors. This section outlines some of the previous work done in the field of calculating the radiative properties of fibrous materials, and analyses the radiative transport across fibrous material.

The beginning of the section gives some references to textbooks dealing with the fundamental aspects of radiative transfer in participating media. Further references on specific subjects are given in the report or in the appendices.

2.1 General theory and approximating methods

Siegel and Howell [1992] describe the general theory of thermal radiation heat transfer including radiative heat transfer in participating media such as fibrous materials. From this book further references can be obtained on various specific areas of the subject radiative transfer. The book also presents a broad overview of different approximations methods for solving the R.T.E.

Several other textbooks are available on the subject of thermal radiation heat transfer. Some are more particularly concerned with the approximations methods to solve the R.T.E. Brewster [1992] treats the fundamental aspect in radiative heat transfer as well as the properties aspect and consider the transfer between surfaces in participating media. Ozisik [1973] treats the various existing solutions methods of the R.T.E. and gives an introduction to the spherical harmonics method.

2.2 Calculation of radiative properties in fibrous materials

When calculating the radiative properties in a particle medium the ratio between the particle size and the wavelength of the radiation must be considered. When the particles are either much smaller or much larger than the wavelength of the radiation different approximations for calculating the radiative properties of the particles are available, which simplifies the problem remarkably.

Table 2.1 shows which theories should be used to calculate the radiative properties of the particles, depending on the particle size and the wavelength spectra, (Siegle and Howell, 1992).

Table 2.1: Theory used for solving radiative properties of particles, depending on the ratio between wavelength and particle size, (Siegel and Howell, 1992).

Ratio between wavelength and particle size	Theory to solve the radiative properties of the particles
$\lambda >> D$	Rayleigh
all	Mie
$\lambda << D$	Fraunhofer and Fresnel diffraction and reflection

Gustav Mie derived mathematically the radiative properties of spheres already in 1908 as the first. The Mie theory is an analytical solution of Maxwell's electromagnetic equations which govern the propagation of electromagnetic waves. Rayleigh scattering is a special case of Mie scattering for small particles compared to wavelength and it is described by much simpler equations than the general Mie theory.

In fibrous materials for building applications the diameter of the fibres and the wavelength of the radiation are of same order of magnitude, and therefore the Mie theory should be used to compute the radiative properties of the fibres.

Kerker [1969] later analytically solved the absorption and scattering of electromagnetic radiation by a single infinitely long cylinder at oblique incident by using the Mie theory. Tong and Gritzo [1993] use Kerker's work for developing their own computer code and obtained the absorption and scattering efficiencies $Q_{a\lambda}$ and $Q_{s\lambda}$ of both spheres and fibres.

Other computer codes of calculating the radiative efficiencies are available in the literature. Bohren and Hoffman [1983] present a computer code concerning a normally illuminated infinite cylinder.

In the available literature either mean radiation coefficients (e.g. obtained by using the Planck function as a weighting function) are used in the R.T.E. or a spectral analysis is performed on the R.T.E.

From the performed survey there seems to be a lack of knowledge concerning the accuracy of using mean properties when modelling radiative heat transfer in fibrous material. However, several authors have discussed the applicability of mean radiative properties in connection with gasses. Viskanta [1964] investigated radiation in an absorbing-emitting gas and obtained integral equations for the mean absorption and emission coefficients; he emphasised that the mean radiative properties cannot be obtained until the spectral solution is known. Viskanta and Mengüc [1987] reviewed the general literature dealing with weighted radiative properties, and further references can be obtained here. However, the results obtained from radiative analyses of gas, e.g. concerning the accuracy of using mean properties, cannot be assumed to be valid also in case of fibrous material since the spectral properties of gases vary much more with the wavelength than those of a dispersed medium of fibres do.

In the main part of the literature the fibres are assumed to be randomly oriented in parallel planes perpendicular to the direction of the heat flux. Lee [1986, 1988, and 1989] treats the calculation of the radiative coefficients of the fibrous materials taking into account the fibre orientation and thus he removes the restriction in the previous analysis that allows the fibres to be either randomly oriented in the space, or in parallel planes only.

2.3 Previous analysis on fibre glass

The two-flux approximation is commonly used to calculate the radiative transfer because of it's simplicity but it has limited accuracy. However, the discrete ordinate method or the spherical harmonics method gives results with arbitrary accuracy for high approximation order obtained at the expense of high computation time.

Tong and Tien [1980, 1983] use a spectral two-flux model to calculate the radiative heat transfer in fibrous material. In the article from [1980] they also give a detailed summary of earlier work done in the field of various radiative diffusive models. While Tong et al. [1990] use the spherical harmonics approximation to analyse the influence of the fibre size on the radiant output of porous radiant burners. In this model they use average radiative properties with Planck's blackbody distribution function as a weighting function. Furthermore, they assume isotropic scattering.

Dombrovsky [1996] also apply a low order spherical harmonics method (P-1) to describe the spectral radiative heat transfer in dense fibrous material using two spectral bands.

Langlais et al. [1995] work with the spectral two-flux model to analyse the impact of different parameters on the radiative heat transfer with focus on the chemical composition of glass. In the article they also reflect on the influence of anisotropy in the fibre orientation on the radiative heat transfer. Their calculations show that the scattering coefficient increases as the orientation becomes more anisotropic. However, they point out that it is very difficult to give an absolute criterion to express the influence of a given parameter on the radiative heat transfer due to the complexity of the problem.

Boulet et al. [1993, 1996] present a spectral discrete multiflux model giving good results. However, at low density of the fibrous material and at room temperature the model systematically underpredicts the thermal conductivity. Houston [1980] uses the discrete ordinate method to analyse spectral radiative transfer applying a band approximation and concludes that the anisotropy of the scattering is very important when modelling the radiative heat transfer.

Banner et al. [1989] use the two-flux mode to calculate the radiative heat transfer when investigating the influence of the temperature in the range from 20°C to 500°C on the optical properties of the fibrous material. They found a good agreement between experimental data and theoretical calculations even though they consider a mono-diameter only. They conclude that a spectral approach is required to calculate the heat transfer in fibrous materials due to the nongray behaviour of the fibres. They also found that the absorption coefficient increases strongly with the temperature whereas the scattering coefficient only varies weakly with the temperature but interference effects occur when scattering at high temperature.

3. Modelling radiative heat transfer in fibrous materials

In this chapter the governing equations for calculating radiative heat transfer in fibrous material are described. Due to the highly spectral dependent radiative properties of the fibrous material, a spectral analysis of the radiative equation is required.

The main problem of calculating radiative transfer in fibrous materials is the radiative transport equation (R.T.E.), which cannot be solved analytically. The two approximation methods to solve the R.T.E., which are compared in appendix A, are introduced in this section together with further references to more detailed information about the methods.

3.1 Physical description of problem

The geometry of the physical problem examined is shown in figure 3.1. The fibrous material is placed between two infinitely parallel plates at different temperatures, which causes a one-dimensional heat flow throughout the specimen. The geometry resembles a standardised test apparatus in (ISO 8302,1991) for measuring apparent thermal conductivity in fibrous materials for building use.

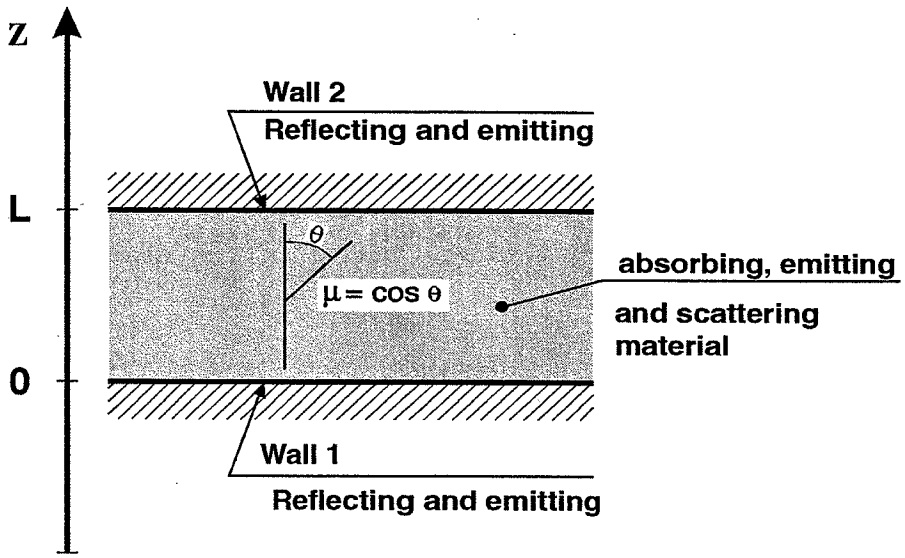

Figure 3.1: Geometry of fibrous material.

In the developed computer model for the heat transfer through the fibrous material, the following assumptions have been made:

- the heat conduction model is one-dimensional and steady-state
- convection in the air between the fibres is disregarded
- the fibrous material is regarded as an absorbing, emitting and scattering medium
- the radiation problem has azimuthal symmetry, which means that the radiative properties of the fibrous material are equal in all directions inside the medium
- the scattering and absorption of the individual fibres are independent
- the fibres are straight, and the optical properties of the bulk glass can be used to characterise the fibres. The optical properties are assumed not to be affected by the binder in the fibrous material
- the boundaries are grey and perfectly diffuse when emitting and reflecting

3.2 Mathematical model – general heat transfer equations

The governing heat transfer equations describing the energy and radiation transfer are coupled by the temperature. The equations presented are derived for a control volume of fibrous material consisting of a gas phase and a fibre matrix phase, assuming steady-state conditions.

Energy conservation equations:

Considering the conservation of energy in the control volume of the gas phase only, the heat transfer is caused by conduction in the gas and by heat exchange between gas and fibres. The effective thermal conductivity of the gas is estimated as a product of the porosity ϕ and the thermal conductivity of the gas itself. Other more sophisticated methods of defining the effective thermal conductivity of the gas phase are given in Houston [1980] and Bankvall [1972]. As this issue was not the main subject of this project the simple relation has been chosen. The energy balance of the gas phase is illustrated in figure 3.2.

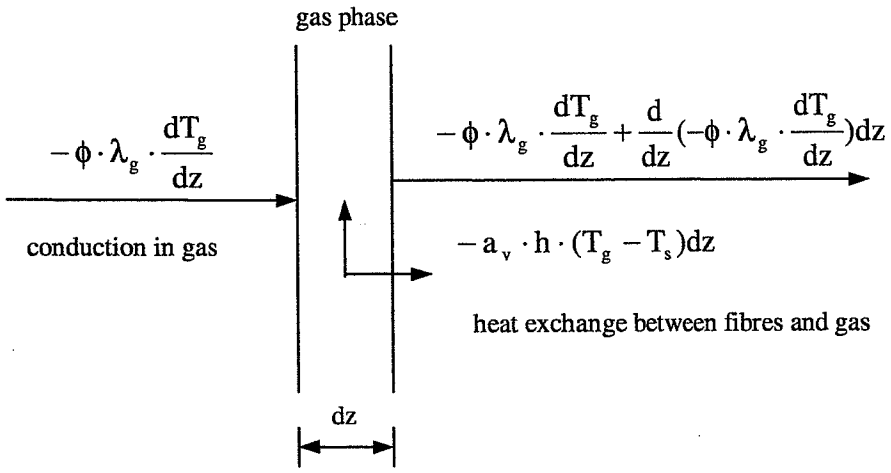

Figure 3.2: Energy balance in a control volume of a gas phase. The left-hand side shows the gain of energy and the right-hand side shows the loss of energy due to conduction and to heat exchange from surface contact between fibres and gas.

According to figure 3.2 the conservation of energy in the gas phase in the steady-state case becomes:

$$-\frac{d}{dz}(\phi \cdot \lambda_g \cdot \frac{dT_g}{dz}) - a_v \cdot h \cdot (T_s - T_g) = 0 \qquad (3.1)$$

Figure 3.3 illustrates the energy balance in the control volume containing the fibre matrix. Here the heat is transmitted by conduction in the fibres, by radiation, and by heat exchange between fibres and gas.

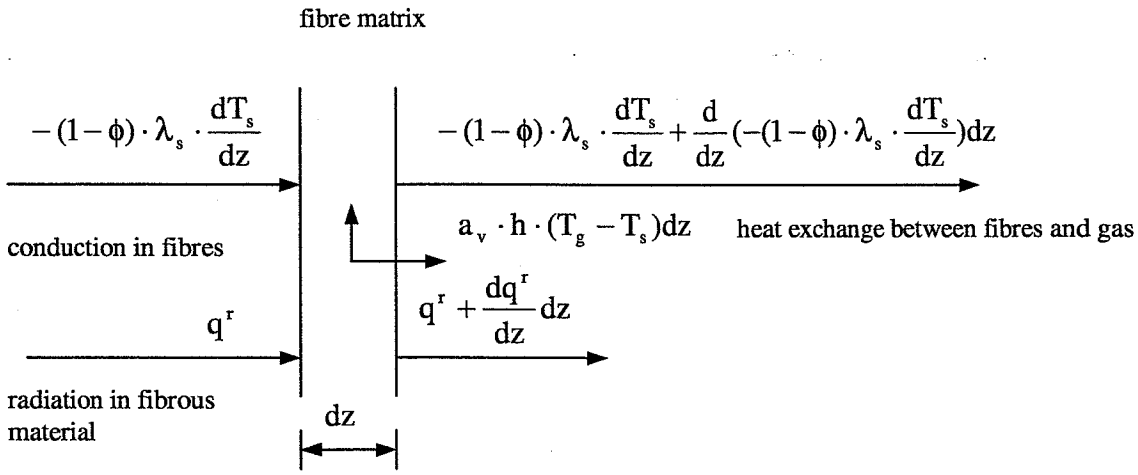

Figure 3.3: Energy balance in a control volume of the fibre matrix. The left-hand side shows the gain of energy, and the right-hand side shows the loss of energy due to conduction in fibres, radiation and heat exchange by surface contact between fibres and gas.

According to figure 3.3 the conservation of energy in the control volume containing the fibre matrix for the steady-state case becomes:

$$-\frac{d}{dz}((1-\phi)\cdot\lambda_s\cdot\frac{dT_s}{dz}) + a_v \cdot h \cdot (T_s - T_g) + \frac{dq^r}{dz} = 0 \qquad (3.2)$$

$(1-\phi)\cdot\lambda_s$ is the effective conductivity of the fibre material which also includes contact resistance.

Equation of radiative transfer:

When radiation passes through the fibrous material, the fibres are interfering with the electromagnetic waves causing changes in the radiative heat flux by scattering, and absorbing the incident radiation and by emission. As the fibres are in the shape of circular cylinders, the scattering must be expected to be non-isotropic. As the optical properties of the fibre material are strongly dependent on the wavelength in the temperature domain considered, a spectral analysis of the radiative flux is required.

In the general case the radiative flux is defined by eq. (3.3):

$$\bar{q}^{r} = \begin{Bmatrix} q_x^r \\ q_y^r \\ q_z^r \end{Bmatrix} = \begin{Bmatrix} \int_{\lambda=0}^{\infty}\int_{\omega=0}^{4\pi} i_\lambda(\theta,\xi) l_x \, d\omega d\lambda \\ \int_{\lambda=0}^{\infty}\int_{\omega=0}^{4\pi} i_\lambda(\theta,\xi) l_y \, d\omega d\lambda \\ \int_{\lambda=0}^{\infty}\int_{\omega=0}^{4\pi} i_\lambda(\theta,\xi) l_z \, d\omega d\lambda \end{Bmatrix} \tag{3.3}$$

in which (l_x, l_y, l_z) is the unit direction vector in the global x, y, z coordinate system. The l_x, l_y, l_z are direction cosine and related to the polar angles as follows:

$$l_x = \sin\theta\cos\xi, \qquad l_y = \sin\theta\cos\xi, \qquad l_z = \cos\theta \tag{3.4}$$

in which the angles θ and ξ are defined according to figure 3.4.

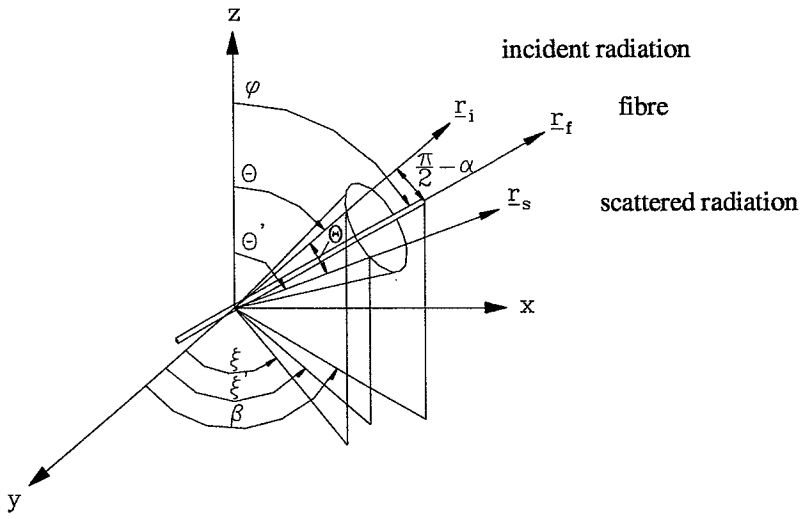

Figure 3.4: Definition of angel notation used in the text.

The R.T.E. eq. (3.5), which describes the change in radiation intensity $di_\lambda(S)$ as the radiation travels the distance S within the absorbing, emitting and scattering medium, is given by (Siegel and Howell, 1992):

$$\frac{di'_\lambda(\bar{S})}{dS} = -\sigma_{a\lambda}\cdot i'_\lambda(\bar{S}) + \sigma_{a\lambda}\cdot i'_{b\lambda}(\bar{S}) - \sigma_{s\lambda}\cdot i'_\lambda(\bar{S}) + \frac{1}{4\pi}\int_{\xi'=0}^{2\pi}\int_{\theta'=0}^{\pi}\sigma_{s\lambda}\cdot i'_\lambda(\bar{S},\theta',\xi')\Phi_\lambda(\Theta)\sin\theta' d\theta' d\xi' \tag{3.5}$$

in which $\sigma_{a\lambda}$ and $\sigma_{s\lambda}$ are the spectral radiative properties of the medium, and Φ is the scattering phase function which is used to model the anisotropic scattering. The determination of the radiative properties of fibrous material are discussed in chapter 4, whereas the

scattering phase function is described in the following with respect to the approximation methods. A survey regarding the scattering phase function can be found in Siegel and Howell [1992].

The individual terms in eq.(3.5) describe:

$-\sigma_{a\lambda} \cdot i'_{\lambda}(\bar{S})$: Loss of intensity by absorption

$\sigma_{a\lambda} \cdot i'_{b\lambda}(\bar{S})$: Gain of intensity due to emission by the medium

$-\sigma_{s\lambda} \cdot i'_{\lambda}(\bar{S})$: Loss of intensity by scattering into other directions

$\frac{1}{4\pi}\int_{\xi'=0}^{2\pi}\int_{\theta'=0}^{\pi}\sigma_{s\lambda} \cdot i'_{\lambda}(\bar{S},\theta',\xi')\Phi_{\lambda}(\Theta)\sin\theta' d\theta' d\xi'$: Gain of intensity by in-scattering in the direction S from all other directions.

In the R.T.E. it has been assumed that the scattered radiation does not change its wavelength upon scattering (i.e. elastic scattering). If this were not a valid assumption, the in-scattering term would have to include an integral over all wavelengths, with Φ serving a dual role of characterising the angular distribution of scattered intensities and radiation transitions from other wavelengths to the one specified for the R.T.E. (Tong and Gritzo, 1993).

The R.T.E. in eq. (3.5) and the energy equation, eq. (3.2), constitute a system of coupled differential equations in which the main difficulty stems from the R.T.E., which is an integro differential equation that cannot be solved analytically.

Only a brief introduction to the two approximation methods, which are compared in appendix A, is presented in the following. A more detailed description of the approximations, including boundary conditions, is given in Dyrbøl [1997] or can be found in textbooks on radiative transfer, e.g. Siegel and Howell [1992], Brewster [1992] or Ozisik [1973].

3.2.1 The two-flux model

Schuster and Schwarzschild proposed the two-flux model in 1905 for studying radiative transfer in stellar atmospheres. The principle of the model is to divide the solid angle about a location into two hemispheres, in which the intensity in positive and negative directions is assumed to be constant, but of different values. If the solid angle is divided into a number of hemispheres each with uniform intensity, the approximation is denoted as the "multiflux" method or discrete ordinate method. The principle of the two-flux model is illustrated in figure 3.5.

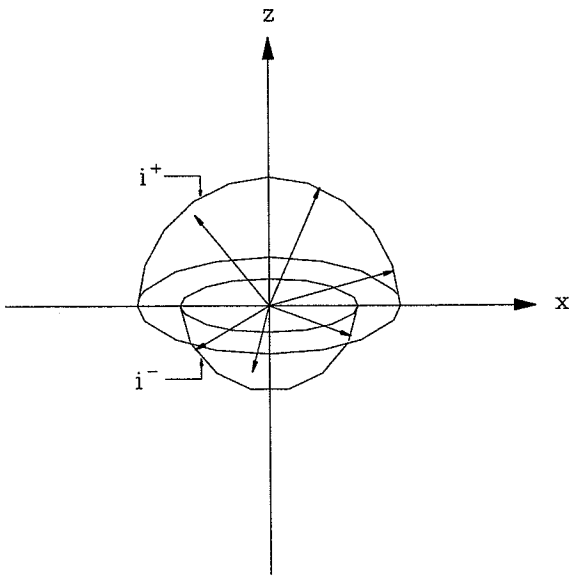

Figure 3.5: Approximation of intensities being isotropic in forward and backward directions.

By dividing the radiation field into a forward and a backward hemisphere with constant intensity ($i^+ = q^+/\pi$ and $i^- = q^-/\pi$, respectively) the R.T.E. is transformed into a pair of ordinary differential equations, eq. (3.6-3.7):

$$\frac{dq_\lambda^+}{dz} = -2(\sigma_{a\lambda} + b_\lambda \sigma_{s\lambda})q_\lambda^+ + 2\sigma_{a\lambda} e_{b\lambda} + 2b_\lambda \sigma_{s\lambda} q_\lambda^- \tag{3.6}$$

$$-\frac{dq_\lambda^-}{dz} = -2(\sigma_{a\lambda} + b_\lambda \sigma_{s\lambda})q_\lambda^- + 2\sigma_{a\lambda} e_{b\lambda} + 2b_\lambda \sigma_{s\lambda} q_\lambda^+ \tag{3.7}$$

in which b_λ is the spectral backscattering factor which, in the two-flux model, is used to model anisotropic scattering. In the computer code developed, b_λ is defined according to Brewster [1992] as the part of the radiation, which is scattered back into the backward direction. The relation between the backscatter factor and the scattering phase function in the R.T.E. becomes, (Brewster, 1992):

$$b_\lambda \equiv \int_{\mu=0}^{1} \int_{\mu'=-1}^{0} \frac{1}{2} \Phi_\lambda(\mu, \mu') d\mu' d\mu \tag{3.8}$$

in which μ is the direction cosine ($\mu = \cos\theta$).

In the energy conservation equation eq. (3.2) the differential of q^r is used. The differential can be obtained by adding eq. (3.6) and eq. (3.7) and integrating over the total wavelength domain as shown in eq. (3.9):

$$\frac{dq^r}{dz} = \int_{\lambda=0}^{\infty} \left(\frac{dq_\lambda^+}{dz} - \frac{dq_\lambda^-}{dz}\right) d\lambda = 4\int_{\lambda=0}^{\infty} \sigma_{a\lambda} e_{b\lambda} d\lambda - 2\int_{\lambda=0}^{\infty} \sigma_{a\lambda} (q_\lambda^+ + q_\lambda^-) d\lambda \tag{3.9}$$

The total heat transfer due to radiation and conduction through the fibrous material can be solved with appropriate boundary conditions and a suitable numerical solutions technique when the radiative properties of the fibrous material $\sigma_{a\lambda}$, $\sigma_{s\lambda}$ and b_λ are known. The used boundary conditions are given in appendix A, and the numerical solutions technique used in the spectral computer code is described in Dyrbøl [1998].

3.2.2 Spherical harmonics method (P-N method)

The spherical harmonics method expands the R.T.E. to form a system of equations. Unfortunately, the procedure provides one less equation than the number of unknowns generated. To overcome this difficulty the intensity is approximated by a series expansion in terms of a truncated sum consisting of "N"-terms of products of known Legendre polynomials P_m, and unknown functions ψ_m. When the series is truncated after one or three terms the method is denoted P-1 or P-3, respectively. According to Ozisik [1973] the intensity, at the location z in the direction μ, can be expanded as follows:

$$i_\lambda(z,\mu) = \sum_{m=0}^{N} \frac{2m+1}{4\pi} \cdot P_m(\mu) \cdot \Psi_{m\lambda}(z) \tag{3.10}$$

The scattering phase function Φ used in the R.T.E. to model the anisotropic scattering gives the probability of scattering of radiation by the medium in any given direction with respect to the direction of the incident radiation beam. The scattering phase function can be obtained from the Mie theory as a function of wavelength, particle diameter, and complex refractive index.

According to Ozisik [1973] the exact Mie scattering phase function in the case of anisotropic scattering in isotropic materials can be obtained by:

$$\Phi_\lambda(\Theta) = \sum_{m=0}^{N} (2\cdot m+1) \cdot f_{m\lambda} \cdot P_m(\mu) \cdot P_m(\mu'), \quad f_{0\lambda} = 1 \tag{3.11}$$

in which f_m are factors modelling anisotropy in the phase function. By using only the first Legendre polynomials in eq. (3.11) the phase function becomes "the linear-anisotropic phase function". In order to accurately represent the phase function of highly forward scattering particles, as many as 100 terms may by required in the series (Mengüc, 1985). In the literature several different approximations which retain the anisotropic characteristic of the exact scattering phase function are available.

By the use of eq. (3.10) and (3.11) the R.T.E. can be written as a system of N differential equations. The solution to the equation system is the unknown functions $\psi_{m\lambda}(z)$ which only depends on the location.

In the solution of the spherical harmonics method the spectral radiative flux $q_\lambda^r(z)$ equals the function $\psi_{1,\lambda}(z)$, whereas the rest of the terms in $\psi_{m\lambda}(z)$ have no physical significance and the divergence used in eq. (3.2) is obtained from:

$$\frac{dq_\lambda^r}{dz} = \frac{d\psi_{1,\lambda}}{dz} \tag{3.12}$$

When the spectral solutions are known the total radiative flux is obtained from eq. (3.13):

$$q^r(z) = \int_{\lambda=0}^{\infty} \Psi_{1,\lambda}(z)d\lambda \tag{3.13}$$

In the computer code the boundary conditions applied for the method of spherical harmonics are the Marshak conditions (Osizik, 1973) obtained using the recurrence equations from Andersen [1997].

The two radiation models use different parameters to model the anisotropic scattering. The two-flux model uses the backscatter factor b_λ, whereas the spherical harmonic uses the parameters $f_{0\lambda}$, $f_{1\lambda}$,...etc. In order to compare the results obtained from the two models a relation between the parameters is obtained, assuming the anisotropic scattering phase function in eq. (3.11) to be linear:

$$\Phi_\lambda(\mu,\mu') = 1 + 3 \cdot f_{1\lambda} \cdot \mu \cdot \mu' \tag{3.14}$$

in which f_1 must be within the limits; $-1/3 < f_1 < 1/3$ in order to avoid negative values of Φ, and μ is the direction cosine ($\mu = \cos\theta$). From the definition of the backscatter factor, eq.(3.8), the following relation between $f_{1\lambda}$ and b_λ can be obtained:

$$b_\lambda = \frac{1}{2} - \frac{3}{8} \cdot f_{1\lambda} \tag{3.15}$$

4. Theoretical determination of radiative properties in fibre materials

4.1 Introduction

In this chapter the methodology for calculating the radiative properties of fibrous materials is described. The radiative properties that appear in the R.T.E. are the absorption coefficient $\sigma_{a\lambda}$, the scattering coefficient $\sigma_{s\lambda}$, and the scattering phase function Φ_λ.

When the particles and the wavelengths are in the same order of magnitude the Mie theory must be used to compute the radiative properties of the particles. The absorption and the scattering of electromagnetic radiation at a specific wavelength by a single infinitely long cylinder at oblique incident have previously been solved analytically by Kerker using the Mie theory. The solution gives the spectral absorption and scattering efficiencies $Q_{a\lambda}$ and $Q_{s\lambda}$, which are used to calculate $\sigma_{a\lambda}$ and $\sigma_{s\lambda}$. An intensive summary of Kerker's solutions is presented in Tong and Gritzo [1993] and will not be discussed further here.

In the present work the computer by T. W. Tong and Gritzo [1993] has been used for calculating the radiative efficiencies. The input data needed for calculating $Q_{a\lambda}(D,\alpha)$ and $Q_{s\lambda}(D,\alpha)$ are the optical properties of the fibre i.e. the complex refractive index of the bulk glass, the fibre diameter D, the wavelength of the radiation λ, and the angle between the fibre and the incident radiation.

The spectral optical properties of the fibre are specified by the complex refractive index $m_\lambda = n_\lambda - k_\lambda \cdot i$, in which n_λ is the index of refraction which determines the propagation speed of the wave travelling through the fibre at a certain wavelength, and k_λ is the index of absorption which determines the decrease of spectral intensity. An example of the complex refractive index of a soda-lime-glass from Hsieh and Su [1979], which has been used in the investigation in appendix A and B, is shown in figure together with the blackbody emissive power spectrum at a temperature of 10°C.

Figure shows that the optical properties of the bulk glass strongly depend on the wavelength and that the main part of the energy is located around the wavelength 6-20 μm when the temperature is 10°C. As the temperature increases the blackbody emissive power spectrum will shift towards shorter wavelengths (in the direction of the visible part of the spectrum).

Boulet et al. [1996] investigated the complex refractive index of a soda-lime-glass at 24°C and 400°C and found almost no temperature influence on the optical properties of the bulk glass, which means that the data measured at room temperature could be used up to a temperature of approx. 400°C without introducing serious error.

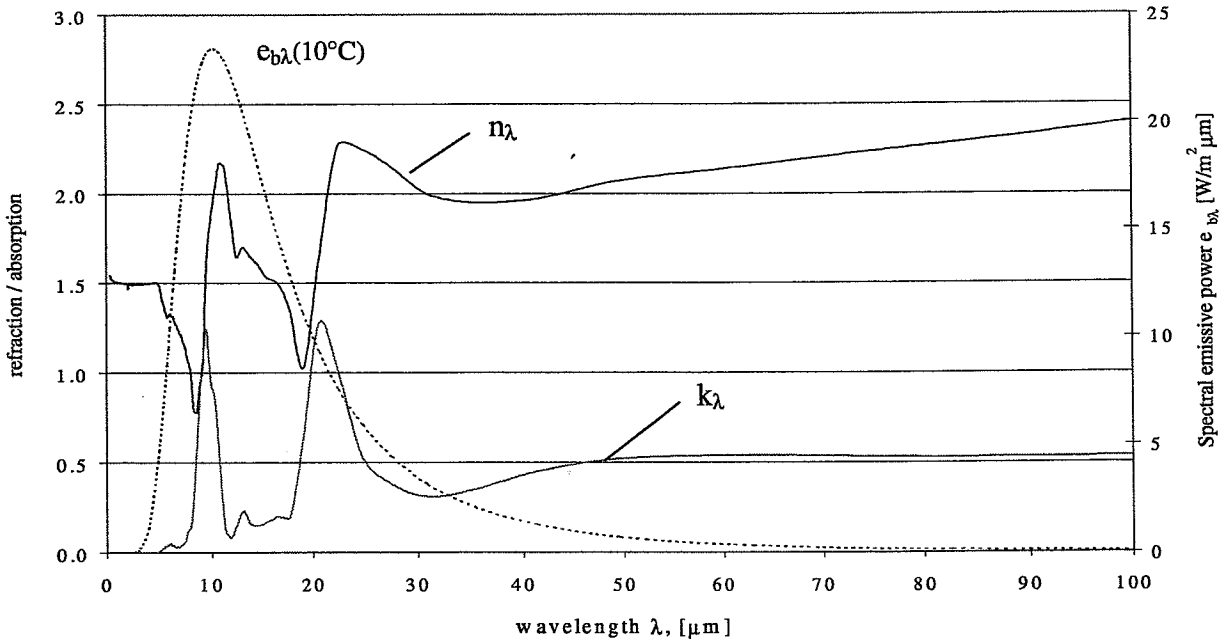

Figure 4.1: Complex refractive index of a soda-lime-silica glass; 73.5w% SiO_2, 21.3w% Na_2O, 5.2w% CaO, according to Hsieh and Su [1979], and the blackbody emissive power spectrum $e_{b\lambda}$ at 10°C.

4.2 Approximating wavelength dependence on optical properties

The wavelength dependence on the optical properties is described by the so-called multi-band model. The electromagnetic spectrum is divided into a number of wavelength bands $[\lambda_i; \lambda_{i+1}]$ in which n_i and k_i are considered as constants. These constant values are calculated by simple averaging, as shown in eq. (3.6):

$$n_i = \int_{\lambda_i}^{\lambda_{i+1}} \frac{n_\lambda d\lambda}{\lambda_{i+1} - \lambda_i} \qquad k_i = \int_{\lambda_i}^{\lambda_{i+1}} \frac{k_\lambda d\lambda}{\lambda_{i+1} - \lambda_i} \tag{4.1}$$

For materials in which the refraction and absorption vary strongly with the wavelength, as in hydroxyl-containing silica glass, a large number of wavelength bands may be required. Petrov [1996] suggests that, on the average, one can assume that a 20-band approximation will be satisfactory in case of strongly wavelength-dependent properties, he found that the calculated absorption coefficient differs by 2.2% between using 33 and 17 wavelength bands at a temperature level of 1100K.

When testing the computer code for calculating the radiative properties in this project the same result was obtained when using 48 as 78 bands, which determined the choice of approx. 40 wavelength bands when different complex refractive index were applied.

4.3 Calculation of scattering and absorption coefficients in fibrous materials

When radiation is incident on a fibre, part of it is reflected and remains in the surrounding medium whereas the rest is transmitted into the fibre. Part of the transmitted energy will be absorbed within the fibre whereas the remaining energy is transmitted into the surrounding medium following one or more internal reflections.

Radiation scattered by a cylindrical fibre proceeds to travel along the surface of a cone, having the fibre as its axis and one side tangent to the incident ray as shown in figure 3., (Lee, 1986).

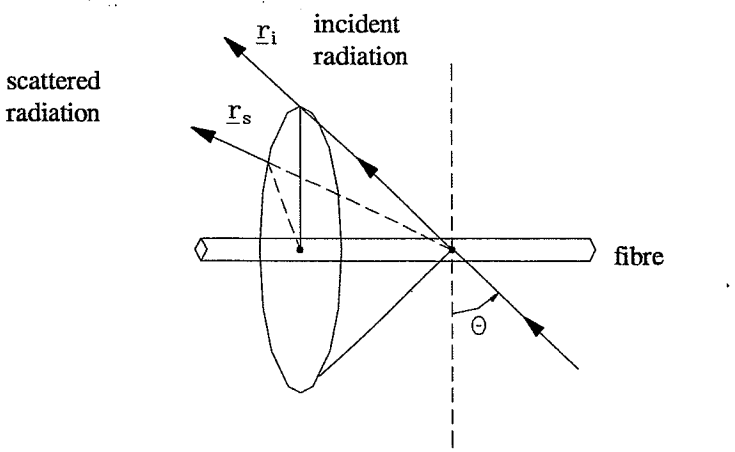

Figure 4.2: Scattering of radiation by a cylindrical fibre according to Lee [1986].

If the scattering behaviour is known for a single fibre, and each fibre scatters independently of the surrounding fibres the scattering coefficient for a cloud of fibres can be obtained using the efficiencies, taking into account the orientation of the fibres, and the fibre diameter distribution.

The conditions for applying independent scattering have been investigated by Hottel et al. [1970] and by Tien and Drolen [1987]. Whether the scattering can be considered as independent depend on the wavelength, the distance between the fibres, and the ratio of this distance to the particle diameter. Figure 3. shows the regions in which independent scattering can be assumed as a function of size parameter $\pi \cdot D/\lambda$ and particle volume fraction f_v.

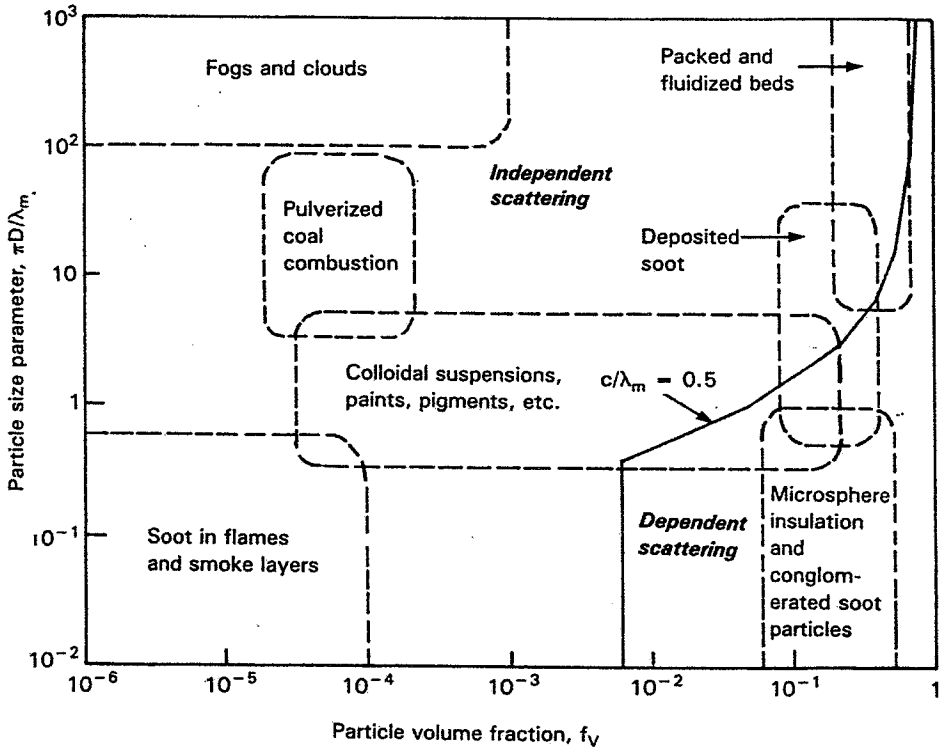

Figure 4.3: Map of independent and dependent scattering regimes as a function of particle size parameter $\pi \cdot D/\lambda$, and particle volume fraction f_v, Tien and Drolen [1987] (reproduced after Siegel and Howell, 1992).

If the volume fraction of the particles f_v is less than approx. $7.5 \cdot 10^{-3}$ independent scattering can be assumed at all particle size parameters ($\pi \cdot D/\lambda$). In low-density fibrous materials f_v is in the range of $3 \cdot 10^{-3}$- $1 \cdot 10^{-2}$, meaning that if the diameter becomes sufficiently small when the particle volume fraction is close to $1 \cdot 10^{-2}$ the assumption about independent scattering may not be valid for all wavelengths, according to figure 3..

However, as the fibrous materials consist of a diameter distribution the average distance between the fibres becomes larger when compared to a mono-diameter material with small diameters. According to Houston [1980], independent scattering may safely be assumed for wavelengths of less than several hundred μm, based on an estimate of the mean distance between the fibres of about 100 μm in typical fibreglass insulation.

Due to the lack of better alternatives independent scattering has been assumed in the following, but one should be aware of possible limitations in the calculations due to this assumption. White and Kumar [1990] show that dependent scattering will decrease the scattering efficiency of parallel fibres at normal incidence, whereas dependent absorption tends to increase the absorption when the particles are small and spherical (Kumar and Tien, 1990).

By specifying the wavelength λ, the fibre diameter D, the angle between the fibre and the incident radiation ($\pi/2-\alpha$), and the spectral optical properties of the fibre one can calculate the radiative efficiencies $Q_{s\lambda}(D, \alpha)$ and $Q_{a\lambda}(D, \alpha)$ of a single fibre.

The radiative efficiencies express the capability of a particle to scatter and absorb radiation per projected area of the particle normal to the incident beam. The scattering and absorption coefficients $\sigma_{s\lambda}$ and $\sigma_{a\lambda}$ represent the collective effect of scattering and absorption from the individual fibres in the volume at a specific wavelength. The scattering and absorption coefficients may be regarded as the reciprocal of the mean free path of the radiation before being scattered or absorbed within the medium.

In spherical particles of uniform diameter D with N_{tot} particles per unit volume the relation between σ_λ and Q_λ becomes very simple, as shown in eq. (3.11):

$$\sigma_\lambda = \frac{\pi \cdot D^2}{4} \cdot Q_\lambda \cdot N_{tot} \tag{4.2}$$

which is valid in case of absorption as well as scattering.

In fibrous materials the relation becomes more complicated, due to the angle between the fibre and the incident radiation ($\pi/2-\alpha$, figure 3.3), which varies depending on the relative direction of the incident radiation and the fibre orientation.

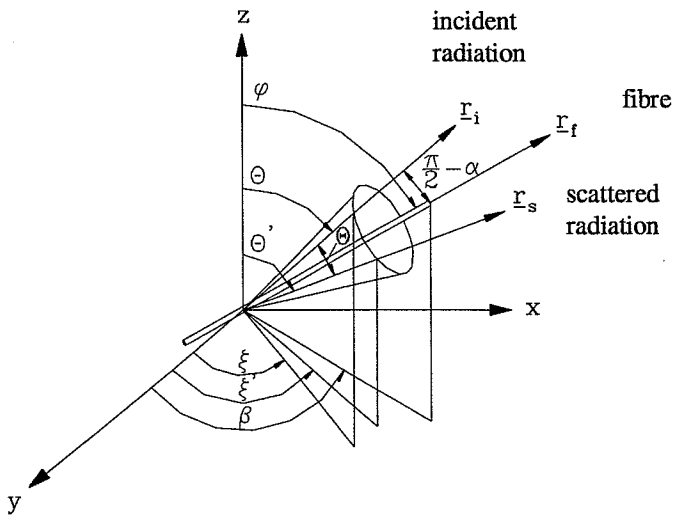

Figure 4.4: Fibre orientation in the space with boundaries parallel to the X-Y plane, according to Lee [1986].

Lee [1986, 1988 and 1989] has investigated the effect of fibre orientation on the radiative properties of a fibrous medium using the angular notation shown in figure3.3. The averaging process of calculating the radiative efficiencies is given in two cases of various fibre orientation distributions:

(a) By assuming the fibres to be randomly oriented in a plane perpendicular to the heat flow direction.

(b) By assuming the fibre orientation in the space to be characterised by a distribution function $f(\beta,\varphi)$.

In case (a), the absorption and scattering efficiencies are averaged using eq. (3.2) and ( ):

$$\overline{Q}_\lambda(D) = \int_0^{\frac{\pi}{2}} Q_\lambda(D,\theta)\sin\theta d\theta \tag{4.3}$$

in which $Q_\lambda(D,\theta)$ is given by eq. ( )

$$Q_\lambda(D,\theta) = \frac{1}{\pi}\int_0^{\pi} Q_\lambda(D,\alpha)d\beta \quad \text{where} \quad \alpha = \left|\arcsin(\cos\beta\sin\theta)\right| \tag{4.4}$$

In case (b), the fibre orientation in the space is assumed to be characterised by a distribution function $f(\beta, \varphi)$ and the absorption and scattering efficiencies $Q_\lambda(D,\theta)$ in eq. (3.2) are going to be calculated from eq. (3.3):

$$Q_\lambda(D,\theta) = \int_{\beta=0}^{2\pi}\int_{\varphi=0}^{\pi/2} Q_\lambda(D,\alpha)f(\beta,\varphi)d\varphi d\beta \quad \text{where} \quad \alpha = \left|\arcsin(\sin\varphi\cos\beta\sin\theta + \cos\beta\cos\varphi)\right| \tag{4.5}$$

The definition of the angles is given in figure 3.2 and the derivation of eq. (3.2-3.3) can be obtained from the literature.

Unfortunately, the distribution of the fibres in the space cannot be measured in the fibrous material. Section 5 describes a preliminary method developed to measure the angular distribution of the two-dimensional texture in fibrous materials. The method may be able to determine an approximation of $f(\beta,\varphi)$.

On the basis of $\overline{Q}_\lambda(D)$ the average values of the scattering and absorption coefficients for a cloud of fibres can be determined taking into account the various fibre diameters characterised by a distribution function f(D), the area of the fibres, and the total number of fibres N_{tot} in a unit volume eq. (3.10):

$$\sigma_{a\lambda} = N_{tot}\int_{D=0}^{\infty}\overline{Q}_{a\lambda}(D)\cdot f(D)\cdot D\cdot l_f(D)dD \tag{4.6}$$

$$\sigma_{s\lambda} = N_{tot}\int_{D=0}^{\infty}\overline{Q}_{s\lambda}(D)\cdot f(D)\cdot D\cdot l_f(D)dD \tag{4.7}$$

The total number of fibre N_{tot} in a unit volume can be obtained by:

$$N_{tot} = \frac{4}{\pi}\cdot\frac{(1-\phi)}{\int_{D=0}^{\infty} D^2\cdot f(D)\cdot l_f(D)dD} \tag{4.8}$$

In fibrous materials the length of the fibres $l_f(D)$ will normally be proportional to the fibre diameter with a proportionality factor of approx. 800 - 1000. In appendix A, two different diameter distributions with a mean diameter of 3.6 μm and 5.7 μm, respectively have been used in the calculations.

4.4 Planck-weighted coefficients

When using weighted radiative properties in the R.T.E. the number of differential equations is considerably reduced compared to the spectral solution. The number of differential equations to be solved depends on the approximation method for solving the R.T.E. If using the weighted radiative properties results in N differential equations a band-model using M bands results in M×N differential equations to be solved.

The frequently applied weighting function for calculating weighted radiative coefficients is the Planck function. The Planck-weighted absorption and scattering coefficients are defined as follows:

$$\bar{\sigma}_{a,Pl} = \frac{1}{\sigma \cdot T_m^4} \int_{\lambda=0}^{\infty} \sigma_{a\lambda} \cdot e_{b\lambda}(T_m) d\lambda \quad \text{and} \quad \bar{\sigma}_{s,Pl} = \frac{1}{\sigma \cdot T_m^4} \int_{\lambda=0}^{\infty} \sigma_{s\lambda} \cdot e_{b\lambda}(T_m) d\lambda \tag{4.9}$$

in which T_m is the mean temperature. The phase function has to be averaged using the spectral scattering coefficient also.

In appendix B the modelling of the radiative heat transfer is compared for the case with the Planck-weighted properties and the spectral properties. The two-flux model is applied in this investigation.

5. Determination of texture in fibrous material

5.1 Introduction

One of the parameters required for calculating the radiative properties of the fibrous material is the orientation distribution of the fibres. The possibility of measuring the orientation distribution of the fibres by way of image analysis has been investigated and is described in Dyrbøl [1996]. Due to the dimension of the fibre 0-20μm, and the porosity of the fibrous material only very few fibres can be measured in each image, thus representing a very small area of the material, figure 5.1. When the aim is to measure the orientation of the single fibre the orientation is three-dimensional whereas the image only shows two dimensions. A huge amount of images is needed to achieve a representative measure of the orientation distribution, even with a large uncertainty from measuring the three-dimensional structure in two dimensions, from measuring the same fibre twice, and from not knowing the exact location of the actual fibre. However, when measuring on a single fibre in image analysis the main difficulty comes from the fibres crossing each other. In image analysis it is not possible to separate the individual fibres.

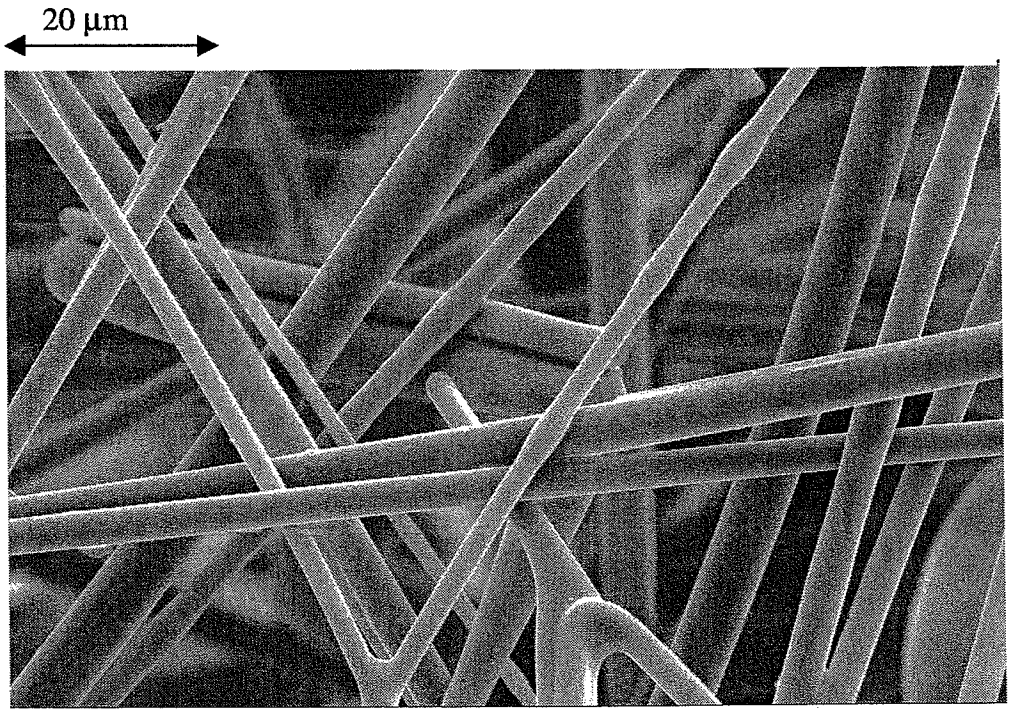

Figure 5.1: Image showing stone wool fibres.

5.2 Method

Instead of measuring the orientation distribution of the single fibres, a method has been developed in collaboration with the Dept. of Mathematical Modelling, DTU, to measure the macro orientation of the texture in the fibrous materials using image analysis. The technique is based on a transformation of the original image into a series of local Fourier transformations. The Fourier transformation models the texture as a series expansion of cosine and sine, and is suitable for identifying structure in images. In the Fourier transformed

image a texture direction in the original image is pictured as a pixel in the directional norm. The distance from the pixel to the centre equals a frequency in the original image. An example of a Fourier transformed image is shown in figure 5.2 (b & c).

The purpose of the method was to estimate:

- the orientation distribution of the dominant orientations in the fibrous material
- the consistency of the measured orientation in the fibrous material

5.2.1 Images

The best way of recording images in the laboratory was to use a flatbed scanner. When using a camera the light must be perfectly diffuse in order to avoid disturbance from the highly reflective fibres. Different resolutions of the images have been tested, and the results are described in Larsen and Hansen [1997].

The image is divided into a number of local windows of equal size in which the dominant fibre orientation in the texture is estimated using Fast Fourier Transformation (FFT). Details about the FFT can be found in textbooks on image analysis, e.g. Russ [1990], and will not be discussed further here.

When imaging fibrous material particularly effects at the boundaries causes disturbances in the FFT image. The sharp edge at the boundaries causes discontinuities in the periodic FFT extension of the window resulting in spectral leakages in the Fourier domain. This phenomenon is often seen as a pronounced "cross" through the centre of the Fourier transformed image (Larsen and Hansen, 1997), the phenomenon is illustrated in figure 5.2 (b).

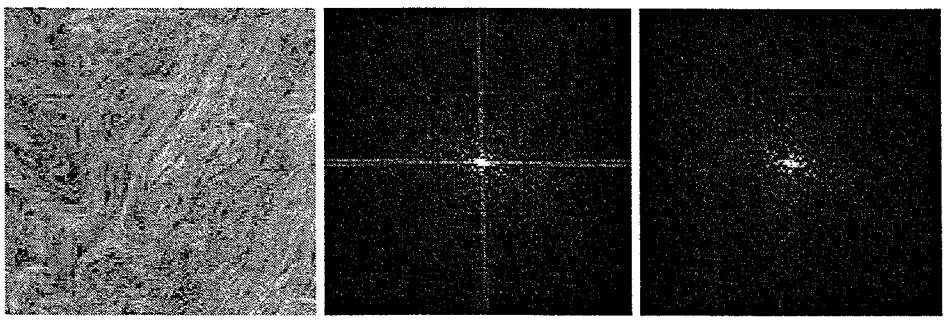

(a) Fibre glass *(b) FFT – no taper* *(c) FFT – with taper*

Figure 5.2: (a) Original image of fibre glass. (b) FFT image of the fibre glass without tapering, discontinuities at the boundaries are seen as a cross through the centre. (c) FFT when image (a) has been multiplied by a taper function which eliminates the discontinuities at the boundaries.

In order to eliminate the cross in the FFT image, the original image (each pixel value in the image) is multiplied by a tapering function. The tapering function is illustrated in figure 5.3, the function is rotationally symmetric and works as a weighting function, which assigns the value "one" to the central area and reduces the influences of the images to "zero" at the boundaries.

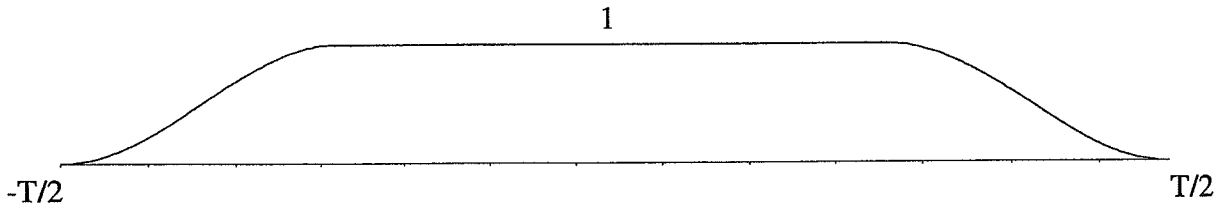

Figure 5.3: Tapering function. T is the pixel size of the window.

The used tapering function w(n) ("Tukey-α-taper" function) is given by eq. (5.1):

$$w(n) = \begin{cases} 1.0, & 0 \le |n| \le (1-\alpha)\cdot T/2 \\ \frac{1}{2}\left[1.0 + \cos\left(\pi \frac{n-(1-\alpha)\cdot T/2}{\alpha \cdot T/2}\right)\right], & |n| > (1-\alpha)\cdot T/2 \end{cases} \tag{5.1}$$

in which T is the pixel size of the local window , α is a factor used to define the area in which w(n)=1 and n is the pixel distance from the image centre. Figure 5.4 shows the resulting image when the local window is multiplied by the tapering function.

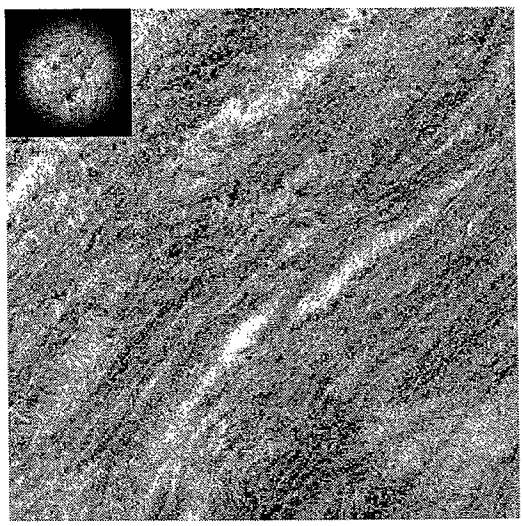

Figure 5.4: Image showing the macro texture in stone wool. The left corner shows the local image multiplied with the tapering function w(n).

In order to achieve as much information as possible from the global image, overlapping local images are applied as shown in figure 5.5.

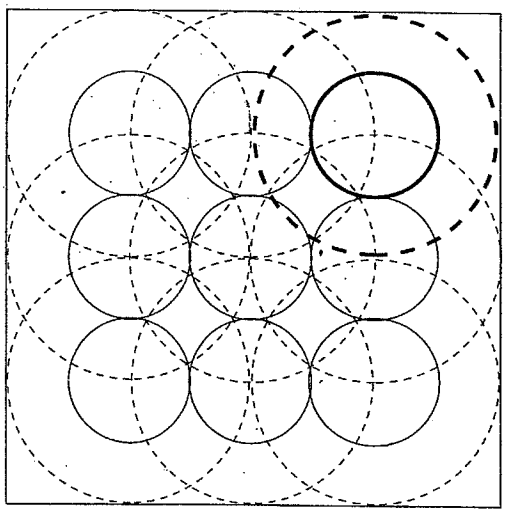

Figure 5.5: The overlap between images is shown by the dotted curves. The overlap in the images does not influence the result, as the weighting function is reduced in this area (reproduced from Larsen and Hansen, 1997).

5.2.2 Determination of dominant orientation

The FFT spectrum in each local image is approximated by an ellipse fitted to the power spectrum centred at (0, 0) as shown in figure 5.6. The dominant orientation of the texture is estimated as the direction of the major axis, **a**, in the ellipsoid. The mathematical description of approximating the FFT with an ellipsoid is shown in appendix C.

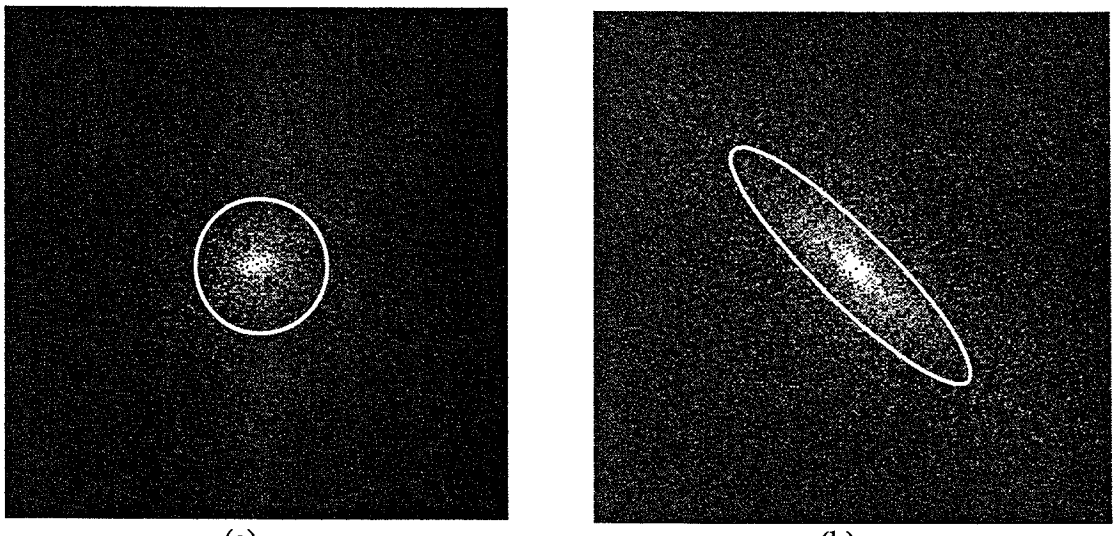

(a) (b)

Figure 5.6: (a) FFT of texture without dominant orientation. (b) FFT of texture with a distinct direction. In both images the ellipsoid approximation is illustrated.

As an estimate of the consistency in the local image, the ratio of the scalar difference between the major axis, a, and minor axis, b, to the major axis is found to be appropriate, eq. (5.2)

$$\text{local consistency} = \frac{a-b}{a} \tag{5.2}$$

If the texture in the image is isotropic the ellipsoid approximation forms a circle and the local consistency becomes zero, as the major and minor axes become equal, figure 5.6 (a). If the texture is perfectly orientated, the minor axis becomes zero and the local consistency approaches unity. In other cases the local consistency of the texture becomes less than one, figure 5.6 (b).

Assuming that the orientation distribution of dominant orientations in the texture reflects the orientation distribution of the single fibres, an estimate of the fibre orientation distribution may be obtained from the distribution of the dominant orientations measured on an appropriate number of the local images.

5.2.3 Determination of orientation distribution – von Mises

Circular data are problematic to analyse due to the wrap-around problem, i.e. 0° and 360° are the same point. However, ordinary linear statistic can be used if the spread of the data is small, and if care is taken to avoid the wrap-around problem, e.g. by displacing the axis.

Special distributions are developed for circular data. One of them is von Mises distribution, which is found to be appropriate when describing the orientation distribution of the dominant orientations measured on the texture in the local images.

The probability density function, similar to the normal distribution of linear data, of an angular random variable θ in the von Mises distribution is:

$$\phi(\theta) = \frac{1}{2\pi I_0(\kappa)} \cdot \exp(\kappa \cos(\theta - \theta_0)) \tag{5.3}$$

in which

θ_0 equals the mean angle in the distribution obtained by vector addition of the measured dominant orientations

κ is a concentration parameter related to the circular variance. κ becomes big if the spread of data is small, and κ becomes small if the spread of data is wide

$I_0(\kappa)$ is the modified Bessel function of the first kind and order 0. $I_0(\kappa)$ can be determined by a polynomial approximation.

In Ersbøll and Conradsen [1998], the method of determining the parameters in eq. (5.3) is described.

By using a known distribution to describe the circular data, it is possible to express mathematically the orientation of the texture in fibrous materials, and to test statistically whether two measured distributions differ form each other significantly.

For numerical calculations the probability of values in the angular interval $p[\theta_i, \theta_{i+1}]$ can be obtained from eq.(5.4):

$$p[\theta_i, \theta_{i+1}] = \int_{\theta_i}^{\theta_{i+1}} \phi(\theta) d\theta \qquad (5.4)$$

5.3 Example of orientation distributions measured on fibrous materials

Figures 5.7 and 5.9 show segments of perpendicular cross sections of a stone wool product and a fibre glass product. Figures 5.8 and 5.10 show the probability density functions according to eq. (5.3), which describe the distributions of the dominant orientations measured on various segments in the same cross section. The mean angles in the probability density functions have been transferred to 0°. In each segment of the cross section the dominant orientation is measured in 161 local images.

The consistency of the dominant orientations has not been taken into account when determining the parameters in the von Mises distribution in figures 5.8 and 5.10. Using an appropriate consistency correction of the measured orientations may improve the method. Furthermore, an investigation of possible disturbance from black regions in the image should be carried out. The black regions, which can be seen in the images in figures 5.7 and 5.9, represent areas without fibrous material in the image.

Table 5.1 shows an overview of the concentration parameters κ in the probability density functions determined for the cross sections in figure 5.7 and 5.9.

Table 5.1: Overview of concentration parameters κ in the probability density functions of the dominant orientations measured on the cross sections shown in figure 5.7 and 5.9.

	Stone wool		**Fibre glass**	
	cross section (a)	**cross section (b)**	**cross section (a)**	**cross section (b)**
	5.3	5.0	10.8	11.9
	7.5	5.7	11.3	7.9
	8.8		9.4	
mean	**7.2**	**5.4**	**10.5**	**9.9**

Although this method is preliminary, and further testing and optimising are required, the method appears promising for describing the texture difference which exists between stone wool and fibre glass. Fibre glass is more directionally orientated than stone wool, which appears as a higher concentration parameter in the fibre glass cross section than in the stone wool cross section.

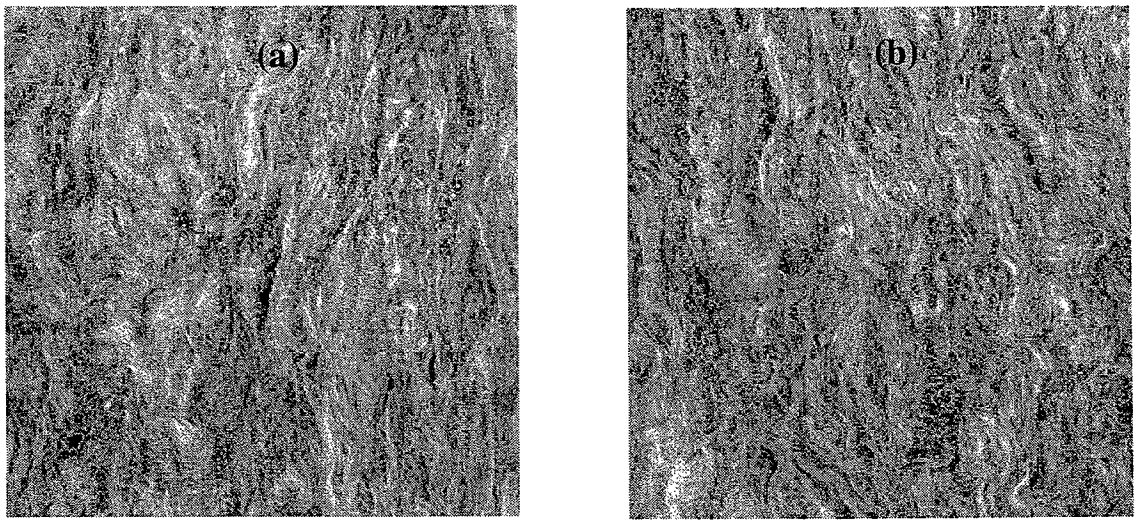

Figure 5.7: Two perpendicular cross sections of stone wool.

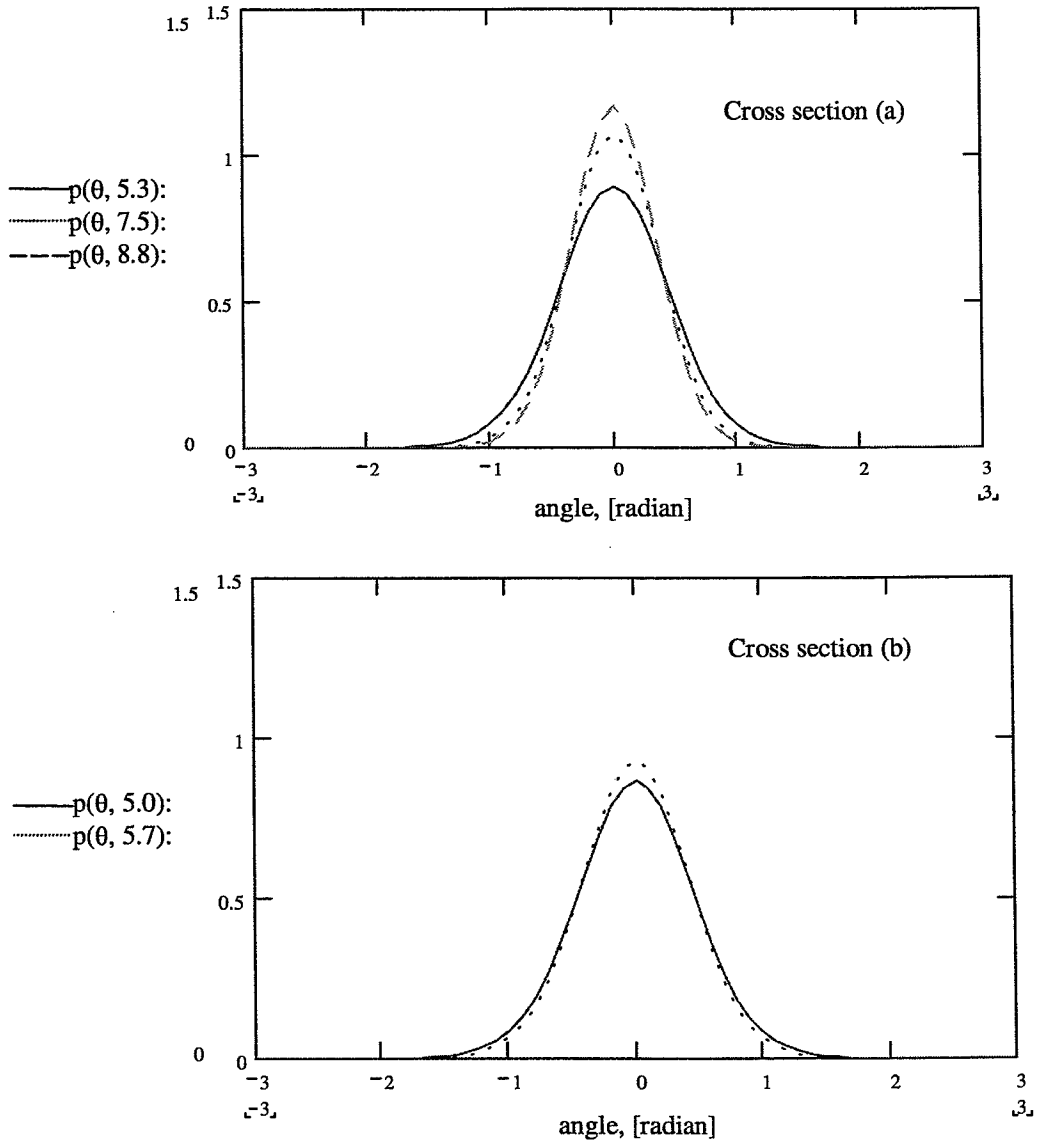

Figure 5.8: Probability density functions of dominant orientations measured on various segments of the cross section (a) and (b) on stone wool. The mean angles have been transferred to 0 radian.

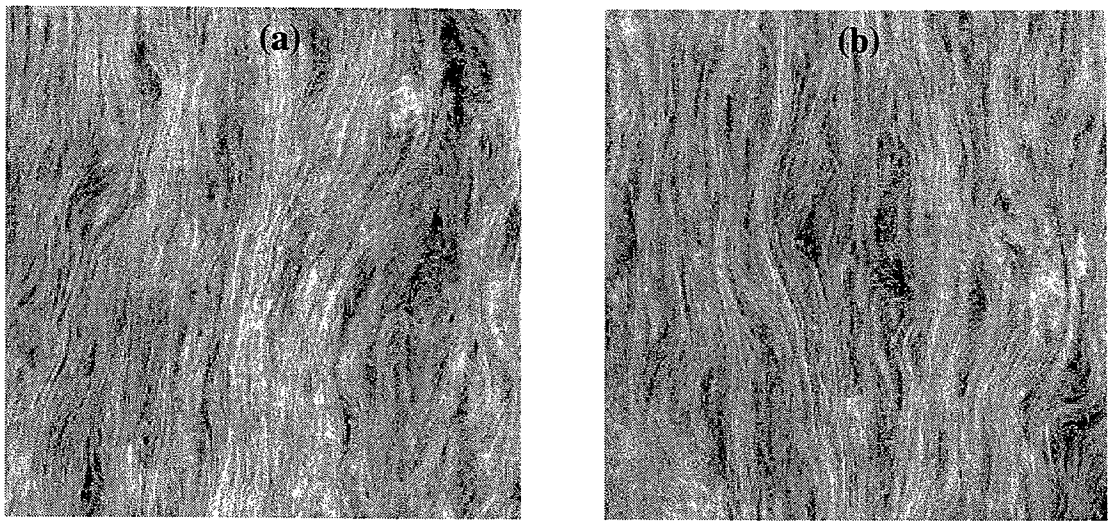

Figure 5.9: Two perpendicular cross section of fibre glass.

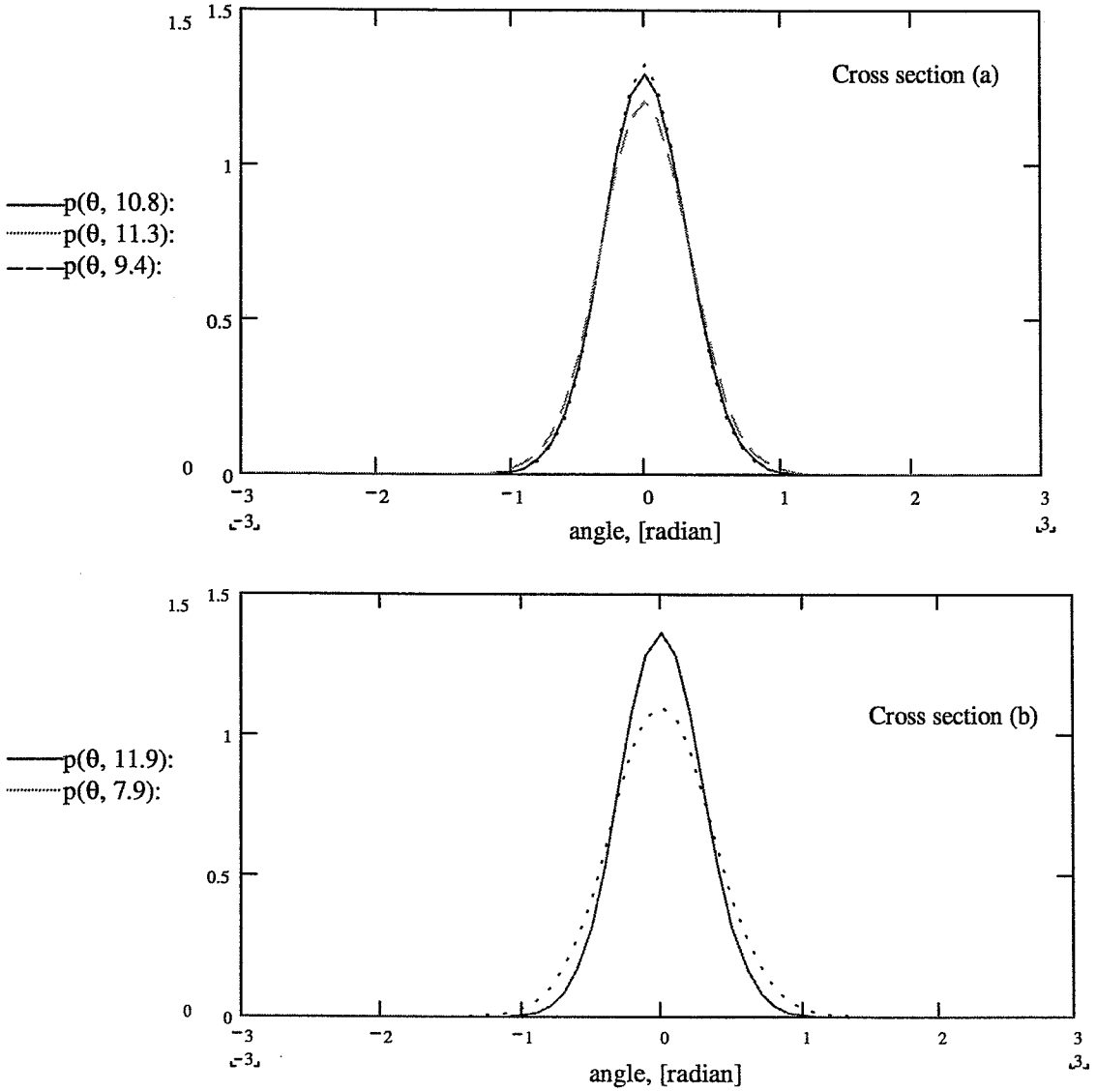

Figure 5.10: Probability density functions of dominant orientations measured on various segments of the cross section (a) and (b) on fibre glass. The mean angles have been transferred to 0 radian.

5.4 Summary

This section presents a preliminary method for determining the orientation distribution in the texture of fibrous materials. The method is based on image analysis using FFT and a statistical distribution concerning circular data.

The orientation distribution of the individual fibres is presumed to be reflected in the visual texture of the fibrous material. Therefor an estimate of the fibre orientation distribution can be obtained on the basis of the method. However, the method is preliminary and not fully developed. Further testing of the method is still required, e.g. in the field of optimising the size of the local windows, eliminating "black" regions in the images, and determining an appropriate correction for the consistency of the measured directions.

6. Conclusion

A computer model for calculating the heat transfer in fibrous materials has been developed. The model includes conduction in gas and fibres, convective heat exchange between the two phases, and radiative heat transfer. The model includes both a two-flux radiation model and the spherical harmonics method with arbitrary high approximation order. In the computer model using the two-flux radiation model a spectral solution of the radiative transport equation can be obtained.

When comparing the two approximation methods comparable input data has been applied in the models, which characterises a typical fibrous material used in the building sector. The Planck-weighted properties of the fibrous material have been used in this investigation.

The performed computations show:

- that the two-flux model underpredicts the radiative heat flux by approx. 15% compared to the accurate spherical harmonics method with arbitrary high approximation order
- that if only the total radiative intensity within the fibrous material is considered, the same results are achieved with the simple spherical harmonics method (P-1) as when using a higher-order approximation of the spherical harmonics
- that the gas and fibre temperatures are the same in both models.

The applicability of the P-1 approximation is limited to cases of moderate anisotropic phase functions. This is an essential limitation when modelling radiation in fibrous materials where the scattering is strongly anisotropic. However, higher-order spherical approximations are able to model a more sophisticated scattering. In order to achieve comparable results the same linear phase function has been used in all the computations.

The two-flux model gives no detailed resolution of the intensity, as it is based on the assumption that the intensities are constant in the two hemispheres. By using a high approximation order of the spherical harmonics, e.g. P-11 or P-21, a detailed resolution of the radiation intensity can been obtained. However, a lower-order approximation i.e. P-1 or P-3 gives much less detailed information concerning the intensity distribution.

An investigation of the accuracy of the radiative flux obtained using the Planck-weighted properties in the two-flux model, compared to the detailed spectral two-flux model, has lead to the following conclusions:

- using the Planck weighted properties underpredicts the radiative heat flux in the centre of the fibrous material by approx. 15% when the porosity is lower than approx. 0.995 and by less at higher porosities.
- it is not possible to determine an appropriate weighting function for calculating weighted radiative properties without knowing the spectral solution, which concurs with the result obtained by Viskanta in 1964 relating to absorption in gasses.

The radiative properties of the fibrous material depend on the morphology of the material. So far it has not been possible to determine the orientation distribution of the individual fibres in the material. This problem still exists – however, a preliminary method for determining the distribution of dominant orientations in the texture of fibrous materials has been developed. By assuming that the orientation distribution of the individual fibres is reflected in the visual texture of the fibrous material, an estimate of the fibre orientation distribution can be obtained by the method presented.

6.1 Recommendations for future work

In this project the two-flux model was found to underpredict the radiative heat flux compared to the spherical harmonics methods when using the Planck-weighted properties. A similar result was obtained using the Planck-weighted properties compared to the spectral properties in the two-flux model. However, from the investigations it is not possible to predict the accuracy in calculated radiative heat flux between the two radiation models when the computations are performed on a spectral basis - this comparison should be done.

In the model independent scattering and absorption were assumed. The validation of this assumption should be investigated further e.g. by experimental work due to the complex problem.

The scattering of radiation in fibrous materials is strongly anisotropic, in the performed investigation a simple model of anisotropic scattering has been applied. This subject is treated in various ways in the literature – however, a way of determining the phase function in fibrous materials needs to be investigated further.

6.2 Commercial perspective

Behind this project were four commercial perspectives:

- to strengthen the Danish research in the area of buildings physics
- to create new collaboration contacts for future projects – national as well as international
- to investigate the effect of natural convection when the material properties approach the limits
- to acquire knowledge of the different heat transport mechanisms to be used in future research for improving the thermal properties of fibrous materials used in the building sector.

The research in the area of natural convection has been initiated in Denmark through this project. At the Department of Building and Energy a new apparatus has been built which will be used in future projects to assess the effects of natural convection in different types of insulation products.

In the project a valuable collaboration has been established with other universities - mainly in the Nordic countries. This will continue after the project.

The results gained in the scientific part of the project are described in the main conclusions in part I and part II, respectively. The knowledge gained through this project will be used by the companies involved in the project in their future research concerning the thermal properties of fibrous materials.

Bibliography

Andersen F. M. B., "Marshak Boundary Condition Recurrence Formula", *Journal of Applied Mathematics and Physics (ZAMP)*, Vol.48 pp.1-6, 1997

Bankvall C. G., "Heat transfer in fibrous materials", National Swedish Building Research, Document D4:1972.

Banner D., Klarsfeld S., Langlais C., "Temperature dependence of the optical characteristics of semitransparent porous media". *High Temperatures – High Pressures*, vol. 21, pp. 347 – 354, 1989.

Bohren, C. F. and Huffman D. R., "*Absorption and Scattering of Light by Small Particles*", Wiley, New York, 1983.

Bomberg M. and Klarsfeld S., "Semi-Empirical Model of Heat Transfer in Dry Mineral Fiber Insulations". *Jour. of Thermal Insulation*, Vol. 6, 1983.

Boulet P., Jeandel G. and Morlot G., "Model of radiative transfer in fibrous media – matrix method". *Int. J. Heat Mass Transfer.* Vol. 36, No. 18, pp. 4287-4297, 1993.

Boulet P., Jeandel G., De Daianous P., Pincemin F., "Combined Radiation and Conduction in Fibrous Insulation (from 24°C to 400°C)", 23th International Thermal Conductivity Conference, Technomic Publishing Co, 1996.

Brewster M. Q., "*Thermal Radiative Transfer & Properties*", John Wiley and Sons, 1992.

Dyrbøl S., "Radiative heat transfer in fibrous materials". Report SR-9812, Dept. of buildings and energy, Technical University of Denmark, 1997. (only available in Danish)

Dyrbøl S., "Program documentation for calculating radiative heat transfer in fibrous insulation". Report SR-9813, Dept. of Buildings and Energy, Technical University of Denmark, 1998. (only available in Danish)

Dyrbøl S., "Billedbehandling og fibermaterialer". Department of Chemistry, Technical University of Denmark 1996. (only available in Danish)

Ersbøll B. K. and Conradsen K., "Analysis of directional data for Rockwool International A/S". Department of Mathematical Modelling, Technical University of Denmark, 1998.

Hsieh C. K., and Su K. C., "Thermal Radiative Properties of Glass from 0.32 to 206 μm", *Solar Energy*, Vol. 22, pp. 37-43, 1979.

Houston R. L. "Combined Radiation and Conduction in a nongray Participating Medium that Absorbs, Emits and Anisotropically Scatters", Ph.D. thesis, Ohio State University, 1980.

Hottel, H. C., Sarofim A. F., Vasalos I. A., Dalzell W. H., "Multiple Scatter: Comparison of Theory with Experiment". *J. Heat Transfer*, vol. 92, no. 2, pp. 285-291, 1970.

ISO 8302:1991E, "*Thermal insulation - Determination of steady-state thermal resistance and related properties - Guarded hot plate apparatus*", 1991.

Kerker M., "*The Scattering of Light and Other Electromagnetic Radiation*", Academic Press, New York, 1969.

Kumar S and Tien C. L., "Dependent Scattering and Absorption of Radiation by Small Particles". *J. Heat Transfer*, Vol. 112, no. 1, pp. 178-185, 1990.

Langlais C., Guilbert G., Banner D., Klarsfeld C., "Influence of the Chemical Composition of Glass on Heat Transfer through Glass Fibre Insulation in Relation to Their Morphology and Temperature use", *Jour. Thermal Insul. and Bldg. Envs.* Vol.18, pp. 350-376, 1995.

Larsen R. and Hansen J. D., "Orientation Analysis of Insulation Materials, A Feasibility Study for Rockwool International A/S". Department of Mathematical Modelling, Technical University of Denmark, 1997.

Lee S. C., "Radiative transfer through a fibrous medium: Allowance for Fiber orientation". *J. Quant. Spectrosc. Radiant. Transfer*, Vol. 36, No. 3, pp. 253-263, 1986.

Lee S. C., "Radiation Heat-Transfer Model for fibers Oriented Parallel to Diffuse Boundaries". *J. Thermophysics*, Vol.2, no.4, 1988.

Lee S. C., "Effect of fiber orientation on thermal radiation in fibrous media". *Int. J. Heat Mass Transfer.* Vol. 32, no. 2 pp. 311-319, 1989.

Mengüc M. P., "Modelling of radiative heat transfer in multidimensional enclosures using spherical harmonics approximation". Ph.D. thesis, Purdue University, 1985.

Ozisik M. N., "*Radiative transfer and interaction with conduction and convection*". John Wiley and Sons, 1973.

Petrov V.A., "Optical and thermophysical properties of semitransparent materials in the calculation of combined radiation and conduction heat transfer". 14th European Conference on Thermophysical Properties, France 1996. High Energy Density Research Center, Institute for High Temperatures, Moscow, Russia.

Pitts D. R. and Sissom L. E., "*Theory and Problems of Heat Transfer*", Schaum's Outline Series, McGraw-Hill Book Company, 1977.

Russ J. C., "*Computer- Assisted Microscopy. The Measurement and Analysis of Images*". Plenum Press, New York, 1990.

Selcuk N., "Evaluation of multi-dimensional flux models for radiative transfer in combustors". Eurotherm proceedings; Heat transfer in radiating and combusting system 2, Italy 1994. Department of Chemical Engineering, Middle East Technical University, Ankara, Turkey.

Siegel R. and Howell J. R., "*Thermal Radiation Heat Transfer*", Hemisphere Publishing Corporation, 3rd. ed., 1992.

Tong T. W. and Tien C. L., "Analytical Models for Thermal Radiation in Fibrous Insulation", *Journal of Thermal Insulation*, Vol.4, pp.27-44, 1980.

Tong T. W. and Tien C. L., "Radiative Heat Transfer in Fibrous Insulation - Part I: Analytical Study". *Journal of Heat Transfer*, Vol.105, pp.70-75, 1983.

Tong T. W., Sathe S. B. and Peck R. E., "Improving the Performance of Porous Radiant Burners through use of Sub-micron size Fibers", *Int. J. Heat Mass Transfer*, Vol. 33, No. 6, pp.1339-1346, 1990.

Tong T. W. and Gritzo L. A., "Mathematical Modelling of Scattering of Radiation in Radiative Heat Transfer", Sandia National Laboratories, Thermal and Fluid Engineering, Dept. 1513, Albuquerque, Development Project 7159.051, 1993.

Tien, C. L and Drolen B. L., "Thermal Radiation in Particulate Media with Dependent and Independent Scattering". *Annual Review of Numerical Fluid Mechanics and Heat Transfer*, vol. 1, pp. 1-32, Hemisphere, Washington, D.C., 1987.

Viskanta R. "Concerning the definition of the mean absorption coefficient". *International Journal of Heat and Mass Transfer*, Vol. 7, pp.1047-1049, 1964.

Viskanta R. and Mengüc M., "Radiation heat transfer in combustion systems". *Prog. Energy Combust. Sci.* Vol 13, pp. 97-160, 1987.

White S. M. and Kumar S., "Interference Effects on Scattering by Parallel Fibres at Normal Incidence". *J. Thermophysics*, Vol. 4, no. 3, pp. 305-310, 1990.

Appendix A:

Andersen, F. and Dyrbøl, S: "Comparison of radiative heat transfer models in mineral wool at room temperature". Presented at: International Symposium on Radiative Transfer, 21 – 25 July 1997, Kusadasi, Turkey.

COMPARISON OF RADIATIVE HEAT TRANSFER MODELS IN MINERAL WOOL AT ROOM TEMPERATURE

F.M.B. Andersen*, S. Dyrbøl**
* Department of Energy Engineering
Technical University of Denmark, 2800 Lyngby, Denmark.
** Rockwool International A/S and Department of Buildings and Energy
Technical University of Denmark, 2800 Lyngby, Denmark.

ABSTRACT. Heat transport in fibrous insulation is modelled, emphasis being placed on radiative heat transfer. The model further includes conductive heat transport in the gaseous and fibrous phases. The case is a planar layer of fibrous insulation with a heated and a cooled plate on the two sides as in a standard test apparatus for measuring the apparent thermal conductivity. The absorption and scattering coefficients are calculated using the Mie theory, a measured statistical fibre diameter distribution, and the orientation of the fibres. The radiative heat transfer is modelled using two models: the two-flux model and the spherical harmonics method with arbitrary approximation order. The system of governing equations is discretized using finite differences and the system of algebraic equations is solved by the Newton-Raphson method. The results show that the radiative heat flux, as well as the radiative conductivity calculated from the two-flux model, is approx. 15 % in error while a P-1 equation gives very accurate results compared to higher order spherical harmonics approximations. The computational costs of low-order spherical harmonics are acceptable, although not as low as when using the two-flux model. The costs of using very high approximation orders such as P-21 are considerable. However, the P-1 and P-3 approximations do not model the angular distribution of the intensity at the walls as precisely as do the P-11 and P-21 approximations.

1. INTRODUCTION

Fibrous insulation is widely used for thermal insulation of machinery and buildings, the aim being to conserve energy and to create acceptable working condition for humans. In cold-climate areas, houses are insulated in order to reduce the cost of heating. Refrigated storehouses are insulated in order to save energy in cooling the rooms. Boilers are insulated partly in order to reduce the surrounding air temperature so that working conditions are acceptable in the boilerhouse, and partly to reduce heat losses. Insulation is used in fire protection of steel structures because insulated steel structures are able to carry a load for a longer periode of time before collapsing. Insulation is also used in other areas, for example to avoid condensation on the outer surface of domestic pipes.

Over the last decade, many projects have been devoted to heat transfer in fibrous material. Houston[1] used the discrete ordinate method to analyse spectral radiative transfer, applying a band approximation, and concluded that accurate modelling of the scattering phase function is very important for accurate results. Tong and Tien[2] used an analytical model to calculate the radiative heat transfer in fibrous material, based on a spectral two-flux model. They also summarized earlier work done on various radiative diffusive models. Langlais et al.[3] have also worked with the spectral two-flux model to analyse the effect of different parameters on radiative heat transfer. Boulet et al.[4] presented a spectral discrete multiflux model which gives good results. However, at low density of the fibrous insulation and at room temperature, the model systematically underestimates the thermal conductivity. Tong et al.[5] used the two-flux model in a combined-mode heat transfer model to

analyse the influence of the fibre size on the radiant output of porous radiant burners. In this model, they used averaged radiative properties where Planck's blackbody distribution function is applied in the averaging process. Furthermore, they assumed isotropic scattering.

It is clear from the above literature investigation that radiative heat transfer is modelled by using either the two-flux model, which is desirable because of its simplicity, or the discrete ordinate method, which can give results with arbitrary accuracy obtained at the expense of a lengthy computational time.

In frequently met cases, the apparent thermal conductivity of fibrous insulation can be expressed by a semi-empirical relation where the apparent thermal conductivity is a function of the porosity (Langlais et al.[3]). These models are able to predict the apparent thermal conductivity when only the porosity is changed but they are useless in many other cases. Therefore, theoretically sound models are required which can predict the effects of changes in parameters such as fibre diameter distribution, fibre orientation distribution or chemical composition of fibre.

In the present paper we supplement the above work and model a layer of fibrous insulation placed between two plates heated to 293.15 K and cooled to 273.15 K respectively (Fig. 1). The geometry of the problem resembles a standardized test apparatus in ISO 8302 [6] for measuring apparent thermal conductivity which includes radiation, conduction in gas and fibre, and convection.

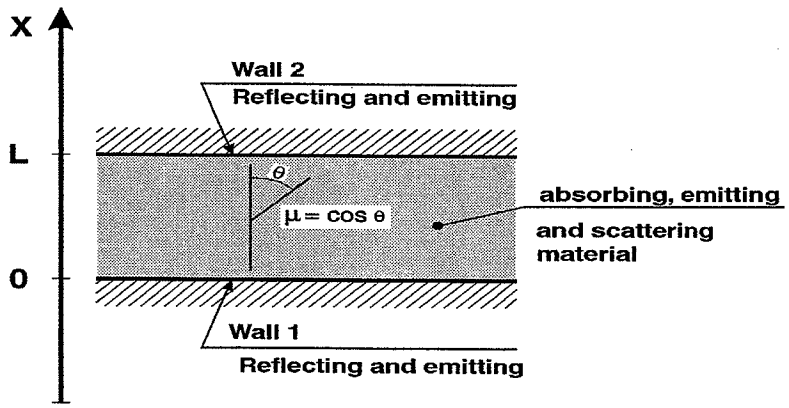

Figure 1. Geometry of the fibrous insulation

This paper presents a heat transfer model which includes two conservation equations for the energy of the gas and the fibres and a number of equations for the radiation exchange, depending on the radiation model and the approximation order. Since radiative heat transfer is significant even at room temperature, and even more important at elevated temperatures, this subject, has received special attention.

The main purpose of this work is to investigate the applicability and the accuracy of the two-flux model in relation to fibrous insulation and to develop a computer code which can be used in future work as a basis for analysing spectral radiative heat transfer. The accuracy of the two-flux model is evaluated by comparison with results obtained using the spherical harmonics method. The applicability of the latter method is investigated.

2. METHOD

Assumptions
The following has been assumed in order to derive the mathematical model:

- The heat conduction model is one-dimensional.
- The gas in the fibrous material is stagnant.
- The radiation problem has azimuthal symmetry .
- The walls are grey and perfectly diffusely emitting and reflecting.

Energy Conservation Equations
The differential equations describing the conservation of energy in the gas and the fibres are:

$$-\frac{d}{dx}(\phi \cdot \lambda_g \cdot \frac{dT_g}{dx}) - a_v \cdot h \cdot (T_s - T_g) = 0 \qquad \text{and} \tag{1}$$

$$-\frac{d}{dx}((1-\phi) \cdot \lambda_s \cdot \frac{dT_s}{dx}) + a_v \cdot h \cdot (T_s - T_g) + \frac{dq^r}{dx} = 0 \tag{2}$$

Fibres and gas are assumed to be in good contact with the walls, giving the following boundary conditions:

$$T_s(0) = T_{w1} \qquad T_g(0) = T_{w1} \qquad T_s(L) = T_{w2} \qquad T_g(L) = T_{w2} \tag{3-6}$$

Two-Flux Radiation Model
In the two-flux radiation model it is assumed that the intensity in the forward and backward hemispheres are constants (Siegel and Howell[7], Tong and Tien[2], Brewster[8]):

$$\frac{dq^+}{dx} = -2 \cdot (\sigma_a + b \cdot \sigma_s) \cdot q^+ + 2 \cdot \sigma_a \cdot \sigma \cdot T_s^4 + 2 \cdot b \cdot \sigma_s \cdot q^- \tag{7}$$

$$-\frac{dq^-}{dx} = -2 \cdot (\sigma_a + b \cdot \sigma_s) \cdot q^- + 2 \cdot \sigma_a \cdot \sigma \cdot T_s^4 + 2 \cdot b \cdot \sigma_s \cdot q^+ \tag{8}$$

The net radiation heat flux is given by $q^r = q^+ - q^-$ and its first derivative applied in eq. (2) is obtained by adding equations (7) and (8):

$$\frac{dq^r}{dx} = \frac{dq^+}{dx} - \frac{dq^-}{dx} = -2 \cdot \sigma_a \cdot (q^+ + q^-) + 4 \cdot \sigma_a \cdot \sigma \cdot T_s^4 \tag{9}$$

The boundary conditions for radiation at the two walls are:

$$q^+(0) = \rho_{w1} \cdot q^-(0) + \varepsilon_{w1} \cdot \sigma \cdot T_{w1}^4 \tag{10}$$

$$q^-(L) = \rho_{w2} \cdot q^+(L) + \varepsilon_{w2} \cdot \sigma \cdot T_{w2}^4 \tag{11}$$

Spherical Harmonics Radiation Model

In the spherical harmonics method the intensity is expanded into a truncated sum of products of Legendre polynomials P_m, and unknowns functions ψ_m, as follows, Ozisik[9]:

$$i(x,\mu) = \sum_{m=0}^{N} \frac{2m+1}{4\pi} \cdot P_m(\mu) \cdot \Psi_m(x) \tag{12}$$

The scattering phase function is given by:

$$\Phi(\mu,\mu') = \sum_{m=0}^{N} (2 \cdot m + 1) \cdot f_m \cdot P_m(\mu) \cdot P_m(\mu') \tag{13}$$

Substituting eq. (12) and (13) into the intego-differential equation describing the radiative transfer equation and applying the orthogonality properties of the Legendre polynomials, the following system of differential equations appears:

$$(m+1) \cdot \Psi'_{m+1} + m \cdot \Psi'_{m-1} + (2 \cdot m + 1)(\sigma_e - \sigma_s \cdot f_m) \cdot \Psi_m = 4 \cdot \pi \cdot \sigma_a \cdot i_b \cdot \delta_{om} \tag{14}$$

for m=0,1,2,..,N-1

$$N \cdot \Psi'_{N-1} + (2 \cdot N + 1)(\sigma_e - \sigma_s \cdot f_N) \cdot \Psi_N = 0 \qquad \text{for m=N} \tag{15}$$

where δ_{om} is the Kronecker delta and prime (') the derivative with respect to location (x).

P_m is a function of the direction cosine $\mu=\cos\theta$ only, and $\psi_m(x)$ is a function of the location x only. $\Psi_1(x)$ is the radiative heat flux and its divergence is applied in eq. (2):

$$\frac{dq^r}{dx} = \frac{d\Psi_1}{dx} \tag{16}$$

The boundary conditions applied for the method of spherical harmonics are the Marshak conditions (Ozisik[9]) obtained using recurrence equations from Andersen[10].

The two radiation models use different parameters to describe the anisotropic scattering. The two-flux model uses the backscatter factor and the spherical harmonics uses the parameters f_0, f_1, .. etc. In order to compare the results obtained from the two models, a relation between the parameters is obtained assuming the linear anisotropic scattering function:

$$\Phi(\mu,\mu') = 1 + 3 \cdot f_1 \cdot \mu \cdot \mu' \tag{17}$$

where $-\frac{1}{3} \le f_1 \le \frac{1}{3}$ in order to avoid negative values of Φ.

Applying the definition of the backscatter factor (Brewster[8]):

$$b = \frac{1}{2} \cdot \int_0^1 \int_{-1}^0 \Phi(\mu,\mu') d\mu d\mu' \tag{18}$$

the relation between f_1 and b is obtained:

$$b = \frac{1}{2} - \frac{3}{8} \cdot f_1 \tag{19}$$

Numerical Solution Technique

The differential equations are discretized by the finite difference technique (Kee et al.[11]). The system of algebraic equations is nonlinear, mainly due to the fourth power of the fibre temperature. The fibre temperature term is linearized in each iteration by the first two terms in a Taylor series and the discretized system is then repeatedly solved using a three-diagonal block matrix solver until convergence is obtained, i.e. Newton-Raphson's method is used.

The computer code which applies the two-flux radiation model uses an equidistant grid, and the number of grid points used in this investigation to give grid-independent solutions are found to be 500. The computer code which applies the spherical harmonics uses an adaptive grid generator involving a gradient criterion only (Kee et al.[11]).

3. INPUT PARAMETERS

The absorption and scattering efficiencies are calculated using the computer code of Tong and Gritzo[12] for a large number of size parameters, $\frac{\pi \cdot D}{\lambda}$, and incident angles of the radiation to the fibre since independent scattering and absorption are assumed. The computer code is valid for infinitely long circular cylindrical fibres with a constant complex refraction index throughout the fibre, i.e. the fibres are not coated or stratified. For glass 1 the complex refractive index from Hsieh and Su[13] is used for 1.0 μm<λ<206.6 μm, and for λ>206.6 μm the index is assumed to be constant. Glass 2 is pure SiO_2 and the complex refractive index from Brewster[8] is used. The absorption and scattering coefficients are then calculated taking into account the diameter distribution and the porosity (Tong et al.[5]), and assuming that the fibres are all randomly oriented parallel to the walls. The calculations of the absorption and scattering coefficients have been checked by comparing the results with the results of Tong and Tien[14] in the case of a monodiameter.

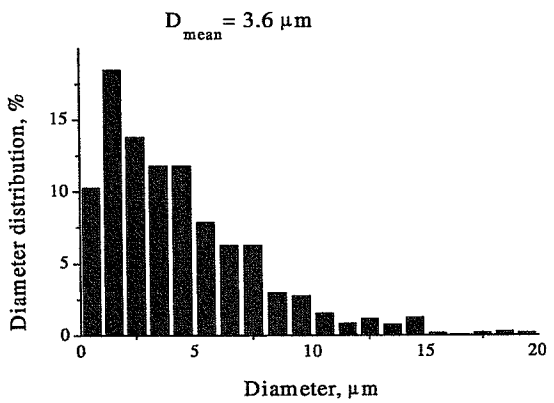

Figure 2. Diameter distribution with D_{mean}= 3.6 μm

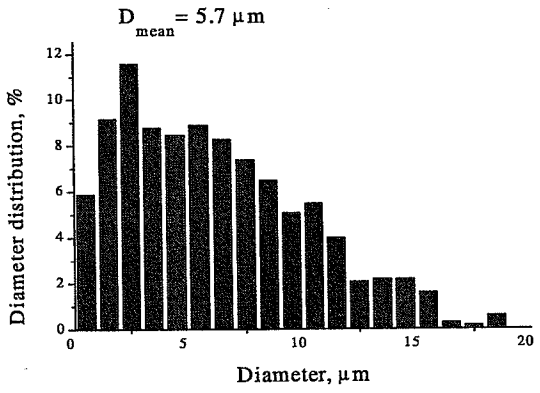

Figure 3. Diameter distribution with D_{mean}= 5.7 μm

The diameter distributions shown in Figs. 2 and 3 are used in the calculations of the radiative properties and the specific surface area of the fibrous insulation (Table 1).

The wall temperatures in the case considered are T_{w1}=293.15 K and T_{w2}=273.15 K, respectively. The emissivity and reflectivity of both walls are ε=0.85 and ρ=0.15, respectively.

TABLE 1
Input Parameters

		Glass 1		Glass 2	
		D_{mean}= 3.6 μm	D_{mean}= 5.7 μm	D_{mean}= 3.6 μm	D_{mean}= 5.7 μm
$\frac{\sigma_s}{1-\phi}$	$[m^{-1}]$	$1.387 \cdot 10^5$	$1.286 \cdot 10^5$	$1.613 \cdot 10^5$	$1.488 \cdot 10^5$
$\frac{\sigma_a}{1-\phi}$	$[m^{-1}]$	$9.573 \cdot 10^4$	$8.730 \cdot 10^4$	$7.790 \cdot 10^4$	$7.040 \cdot 10^4$
b		0.2538	0.2220	0.3201	0.2863
$\frac{a_v \cdot h}{1-\phi}$	$[Wm^{-3}K^{-1}]$	$942 \cdot 10^6$	$942 \cdot 10^6$	$942 \cdot 10^6$	$942 \cdot 10^6$
f_1		0.3283	*0.3333	0.2399	0.2849
Note: * = the value is truncated in order to avoid negative value of Φ.					

The conductivities of the gas and fibres have been expressed as least mean square polynomials of the respective temperatures in the range 273.15 K to 873.15 K. Numerical calculations using the two-flux model show that since the temperature variation in the cases considered is 20 K only, the conductivities at the mean temperature, 283.15 K, can be used without changing the results, i.e. constant conductivity can be used.

It is a well known fact that the conductivity of fibres to be applied in the numerical model is not the value of the fibre material, but an effective value depending on the orientation of the fibres. Fibres orientated orthogonally to the walls have a much greater effective conductivity than fibres parallel to the walls. The effective conductivity of the fibres is calculated from a correlation for fibres parallel to the walls from Bankvall[15].

The heat transfer coefficient, h, is estimated from a correlation valid for a free fine wire due to lack of more appropriate correlations for natural convection inside fibrous media. The surface area of the fibre per volume, a_v, is calculated using the statistical diameter distribution and the porosity. However, due to the great uncertainty of the volumetric heat transfer coefficient, $h \cdot a_v$, it has been varied from $0.01 \cdot h \cdot a_v$ to $100 \cdot h \cdot a_v$, where $h \cdot a_v$ is the value of Table 1, no changes in the radiative heat flux or the gas and fibre temperatures were observed.

4. NUMERICAL RESULTS AND DISCUSSION

For a one-dimensional layer with constant conductivity, the temperature profile is shown to be linear in elementary textbooks. The fibre temperature profile obtained by detailed numerical analysis for glass 1 and the properties in Table 1 for a mean diameter of 3.6 μm deviates slightly from the linear profile as is shown in Figs.4 and 5. When the two-flux model and the P-3 approximation are applied, the maximum deviation from the linear temperature profile is approx. 0.2 K and 0.1 K, respectively. The small deviations are due to the low temperature level and the relatively small temperature difference (20 K) over the fibrous layer.

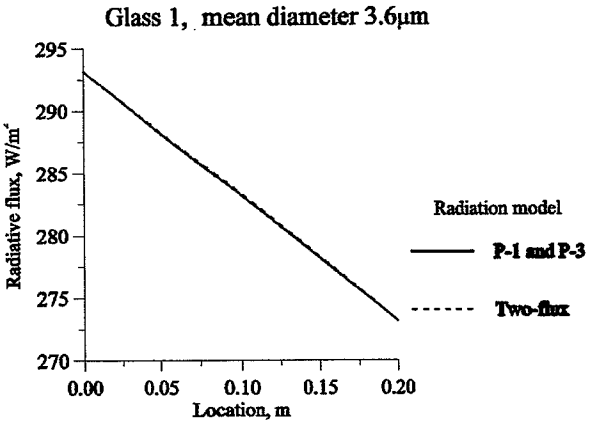

Figure 4. Fibre temperature distribution

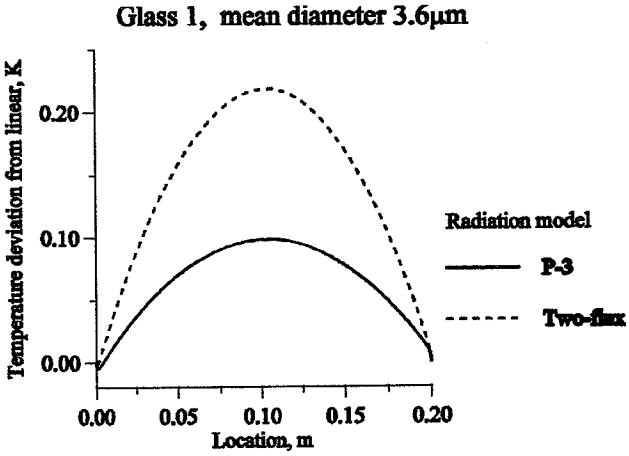

Figur 5. Difference between calculated fibre temperature and linear temperature profile between the wall temperatures

The effective conductivity of radiation in the fibrous material is defined as:

$$\lambda_{eff}^{r} = \frac{-q^{r}}{\frac{dT_S}{dx}} \tag{20}$$

similar to the conductivity of solids and gases. However, the radiative conductivity depends to a great extent on the temperature level that can be seen by comparing the definition in eq. (20) to a radiative diffusion law such as the Rosseland diffusion law.

Table 2 shows the radiative conductivities calculated using the two-flux model and the P-1 and P-3 approximations at a temperature of 283.15 K in the middle of the thermal insulation. It is seen that the errors of the two-flux model vary from approx. 10 % to 17 % compared to the P-3 approximation, which is considered accurate concerning the radiative heat flux since it gives the same values as the P-1 approximation. In the case of glass 1, D_{mean} = 5.7 μm, the value of f_1 is truncated in order to avoid negative value of Φ, i.e. the assumed linear scattering function is not able fully to model the anisotropic scattering in this occasion.

TABLE 2
Calculated Radiative Conductivity for Fibrous Material with a Porosity of 0.9937 and a mean Temperature of 283.15 K.

Material	Mean diameter [μm]	Two-flux [mW/mK]	Spherical harmonics [mW/mK]		Difference: Two-flux and P3
			P-1	P-3	
Glass 1	3.6	4.94	5.80	5.80	14.8%
	5.7	5.69	6.33	6.33	10.1%
Glass 2	3.6	4.53	5.46	5.46	17.0%
	5.7	5.28	6.20	6.20	14.8%

From Fig. 6 it is seen that the two-flux radiative model underpredicts the radative heat flux by approx. 15% in the case of glass 1 with D_{mean}=3.6 μm, while the spherical harmonics method gives

very accurate results even for low-order approximations such as the P-1 and P-3 approximations. The P-11 and P-21 approximations give the same radiative heat flux as those for P-1 and P-3. Since both the two-flux model and the P-1 approximation each give two first-order ordinary differential equations and thus are equally complex, the P-1 must be preferred since it models the radiative heat flux more accurately. However, a drawback of the P-1 approximation is that the anisotropy factor, f_1, must be within the limits $-\frac{1}{3} \leq f_1 \leq \frac{1}{3}$ i.e. only moderately anisotropic scattering can be modelled. The two-flux model is able to model more extreme cases of forward or backward anisotropical scattering.

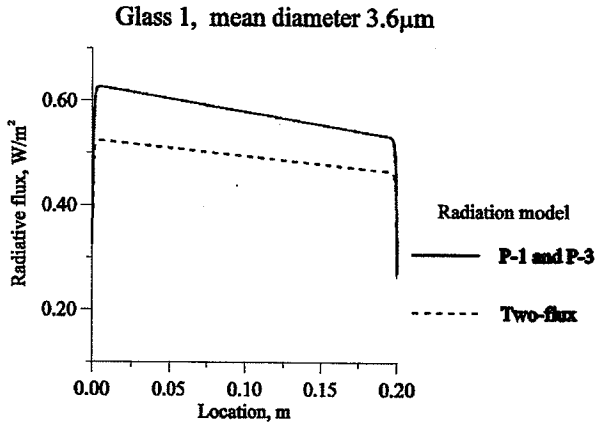

Figure 6. Radiative heat flux calculated using the two-flux model and the spherical harmonics model

The contributions to the apparent conductivity from radiation and conduction in fibres and gas are shown for glass 1 in Fig. 7. The figure is calculated using the P-3 approximations with the thermo-physical properties of Table 1. The radiation at ambient temperatures contributed about 20% to the total apparent conductivity while the gas conduction is dominant with approx. 79%. The conduction in the fibres contributes with approx. 1% only.

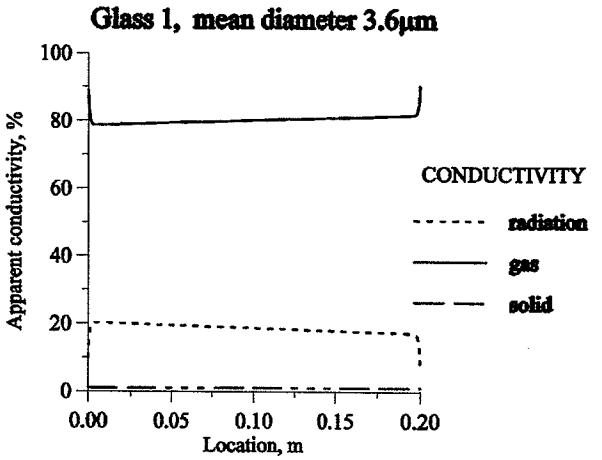

Figure 7. Contributions to the conductivity from radiation and conduction in fibres and gas

The calculated apparent conductivity in the middle of the fibrous insulation does not vary with the emissivity of the walls when the emissivity is varied from 0 to 1 which is to be expected since the material considered is optically thick.

As explained above, the two-flux model underestimates the radiative flux compared to the spherical harmonics method. The errors can be analysed by the radiative diffusion equations derived from the two-flux model and the P-1 approximation in the optically thick limit.

The diffusion equation and the effective conductivity derived from the two-flux model are:

$$q^r_{TF} = -\frac{4\cdot\sigma}{\sigma_a+2\cdot b\cdot\sigma_s}\cdot T_s^3\cdot\frac{dT_s}{dx} \quad \text{and} \quad \lambda_{eff,TF} = \frac{4\cdot\sigma}{\sigma_a+2\cdot b\cdot\sigma_s}\cdot T_s^3 \tag{21,22}$$

and the diffusion equation and the effective conductivity derived from the P-1 approximation are:

$$q^r_{P-1} = -\frac{16\cdot\sigma}{3\cdot(\sigma_e-f_1\cdot\sigma_s)}\cdot T_s^3\cdot\frac{dT_s}{dx} \quad \text{and} \quad \lambda_{eff,P-1} = \frac{16\cdot\sigma}{3\cdot(\sigma_e-f_1\cdot\sigma_s)}\cdot T_s^3 \tag{23,24}$$

In Table 3, the two effective radiative conductivities in eqs. (22) and (24) are compared to the effective conductivities calculated from the numerical solutions using eq. (20).

TABLE 3
The Radiative Conductivity of eq. (22) and (24) Compared to the Numerical Solution

		Effective radiative conductivity [mW/mK]			
		Two-flux		P-1 approximation	
		Numerical solution	Diffusion equation	Numerical solution	Diffusion equation
Glass 1	D=3.6μm	4.94	4.94	5.80	5.80
	D=5.7μm	5.69	5.69	6.33	6.33
Glass 2	D=3.6μm	4.53	4.53	5.46	5.46
	D=5.7μm	5.28	5.28	6.20	6.19

It should be noted that the applicability of the diffusion equation in eq. (21) based on the P-1 approximation is limited to cases of moderate anisotropic phase functions while numerical solutions of higher-order spherical approximation can model strong forward or backward scattering.

It is concluded from the values of Table 3 that the thermal conductivities in the middel of the fibrous insulation may be obtained from the diffusion laws for optically thick materials instead of detailed numerical modelling.

In the above calculations (Table 3) using the diffusion equation, the Planck mean radiative properties have been applied, although the generalized Rosseland mean values should have been applied, defined as follows:

$$\frac{1}{\sigma_a+2\cdot b\cdot\sigma_s} = \int_0^\infty \frac{1}{\sigma_{a\lambda}+2\cdot b_\lambda\cdot\sigma_{s\lambda}}\cdot\frac{\partial e_{\lambda b}}{\partial e_b}\cdot d\lambda \quad \text{and} \quad \frac{1}{\sigma_e-f_1\cdot\sigma_s} = \int_0^\infty \frac{1}{\sigma_{e\lambda}-f_{1\lambda}\cdot\sigma_{s\lambda}}\cdot\frac{\partial e_{\lambda b}}{\partial e_b}\cdot d\lambda \tag{25,26}$$

Equations (25) and (26) are derived parallel to the Rosseland mean extinction coefficient (Siegel and Howell[7]).

Figure 8 shows the intensity as a function of the direction cosine at wall 1. Since the wall is assumed to be perfectly diffusely emitting and reflecting, the intensity from wall 1, i.e. $0<\mu<1$, is constant; the P-11 and P-21 approximations model this very well. The P-1 is too simple an approximation to describe these fine details at the wall, since it assumes a linear distribution of the intensity as a function of the direction cosine, μ. However, the P-1 approximation models the radiative heat flux accurately, as shown above. The P-3 approximation gives much more information than the P-1 as regards the intensity distribution, but is not as detailed as the P-11 and P-21. The intensity to wall 1, i.e. $-1<\mu<0$, is an increasing function of the direction cosine and is modelled with very good accuracy by the P-3, P-11 and P-21. The P-1 again resolves fewer details.

In the derivation of the two-flux model it was assumed that the intensities in the forward and backward hemispheres were constants, i.e. there is a discontinuity at $\mu=0$. That means that the intensity is $i=\frac{q^+}{\pi}$ for $0<\mu<1$ and $i=\frac{q^-}{\pi}$ for $-1<\mu<0$; these values are shown in Fig. 8. It is seen that the two-flux model underestimates slightly the intensities in both hemispheres with less than 0.1%. Because of its simplicity, the two-flux model is not able to give detailed informations concerning the intensity distribution at the wall.

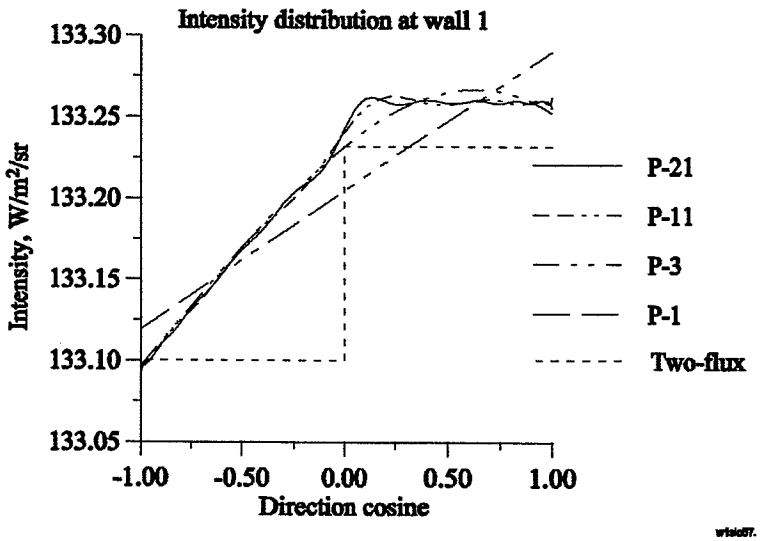

Figure 8. Intensity at wall 1 as a function of the direction cosine, glass 2, D_{mean}= 5.7 μm

5. CONCLUSION

A computer model for the heat transfer in fibrous insulation has been developed and includes models for conduction in gas and fibres, convective heat exchange between the two phases, and radiative heat transfer. The model includes both a two-flux radiation model and the spherical harmonics method with arbitrary high approximation order.

The computations show that the gas and the fibre temperature are the same. The two-flux model underpredicts the radiative heat flux by approx. 15% compared to the accurate spherical harmonics solution, while the P-1 approximation is found to be accurate.

The effective radiative conductivity, based on radiative diffusion equations and detailed numerical calculations, is compared for the two-flux model and the P-1 approximation for a central location inside the fibrous insulation. The detailed numerical modelling and the diffusion approximations give the same results using the Plank's mean value for the radiative properties for the investigated cases which are all optically thick. The applicability of the diffusion equation based on the P-1 approximation is limited to cases of moderate anisotropic phase functions while numerical solutions of higher-order spherical approximation are able to model more sophisticated scattering.

A detailed resolution of the intensity as a function of the direction cosine at a wall has been obtained using a P-11 and a P-21 approximation while a P-1 or P-3 approximation gives much less detailed information concerning the intensity distribution. The two-flux model gives no detailed resolution since it is based on the assumption that the intensities are constants in the two hemispheres.

ACKNOWLEDGMENT

The authors would like to thank Professor T.W. Tong for sharing the computer code for calculating the radiative efficiencies.

NOMENCLATURE

a_v	surface area of fibres per m^3 fibre material [m^{-1}]
b	backscatter factor
f_m	factor in expression of the phase function
h	heat transfer coefficient [$W/m^2/K$]
i	total intensity [$W/m^2/sr$]
L	thickness of the fibre layer [m]
N	order of spherical harmonics approximation
$P_m(\mu)$	Legendre polynomials [m]
q	radiative heat flux [W/m^2]
T	temperature [K]
x	location [m]

Greek letters

ε	emissivity of wall
ϕ	porosity
λ	thermal conductivity [W/m/K]
μ	direction cosine
θ	angle to x-axis
ρ	reflectivity of wall
σ	Stefan-Boltzmann constant: 5.6705110^{-8} W/m^2K^4
σ_a	absorption coefficient [m^{-1}]
σ_s	scattering coefficient [m^{-1}]
σ_e	extinction coefficient [m^{-1}]
τ	optical thickness ($\sigma_e \cdot x$)
Φ	scattering phase function
$\Psi_m(\tau)$	function in the spherical harmonics [$W/m^2/sr$]

Subscript

r	radiation
s	solid
g	gas
b	blackbody
TF	two-flux
P-1	P-1 approximation
w1	wall 1
w2	wall 2
λ	wavelength
+/-	positive/ negative direction of x-axis
i, m	integer

6. REFERENCES

1. Houston R.L."*Combined Radiation and Conduction in a nongray Participating Medium that Absorbs, Emits and Anisotropically Scatters*", Ph.D. thesis, Ohio State University, 1980.
2. Tong T.W.and Tien C.L., "Analytical Models for Thermal Radiation in Fibrous Insulations", *Journal of Thermal Insulation*, Vol.4, pp.27-44, 1980.
3. Langlais C., Guilbert G., Banner D., Klarsfeld C.,"Influence of the Chemical Composition of Glass on Heat Transfer through Glass Fibre Insulations in Relation to Their Morphology and Temperature use", *Jour. Thermal Insul. and Bldg. Envs.* Vol.18, pp. 350-376, 1995.
4. Boulet P., Jeandel G., De Daianous P., Pincemin F.," Combined Radiation and Conduction in Fibrous Insulation (from 24°C to 400°C)",*23 th. ITCC*, Technomic Publishing Co, 1996.
5. Tong T.W., Sathe S.B. and Peck R.E., "Improving the Performance of Porous Radiant Burners through use of Sub-micron size Fibers", *Int. J. Heat Mass Transfer*, Vol. 33, No. 6, pp.1339-1346, 1990.
6. ISO 8302, "Thermal insulation - Determination of steady-state thermal resistance and related properties - Guarded hot plate apparatus", 1991.
7. Siegel R. and Howell J.R., "*Thermal Radiation Heat Transfer*", Hemisphere Publishing Corporation, 3rd. ed., 1992.
8. Brewster M.Q.,"*Thermal Radiative Transfer & Properties*", John Wiley and Sons, 1992.
9. Ozisik M. N., "*Radiative transfer and interaction with conduction and convection*", John Wiley and Sons, 1973.
10. Andersen F. M.B.,"Marshak Boundary Condition Recurrence Formula", *Journal of Applied Mathematics and Physics (ZAMP)*, Vol.48 pp.1-6, 1997
11. Kee F.J., Grcar J.F., Smooke M.D., Miller J.A., "*A Fortran Program for Modeling Steady Laminar One -Dimensional Premixed Flames*", SANDIA REPORT SAN85-8240, Dec 1985.
12. Tong T.W. and Gritzo L.A.,"*Mathematical Modeling of Scattering of Radiation in Radiative Heat Transfer*", Sandia National Laboratories, Thermal and Fluid Engineering, Dept. 1513, Albuquerque, Development Project 7159.051, 1993.

13. Hsieh C.K., and Su K.C., "Thermal Radiative Properties of Glass from 0.32 to 206 μm", *Solar Energy*, Vol. 22, pp. 37-43, 1979.

14. Tong T.W. and Tien C.L., "Radiative Heat Transfer in Fibrous Insulations - Part I: Analytical study", *Journal of Heat Transfer*, Vol. 105, pp.70-75, 1983.

15. Bankvall C.G., "*Heat transfer in fibrous materials*", National Swedish Building Research, Document D4:1972.

Appendix B:

Andersen, F. and Dyrbøl, S: "Modelling radiative heat transfer in fibrous materials: the use of Planck mean properties compared to spectral and flux-weighted properties". Accepted for publication in "Journal of Quantitative Spectroscopy & Radiative Transfer", 1997.

Accepted for publication in Journal of Quantitative Spectroscopy and Radiative Transfer, 1997

Modelling Radiative Heat Transfer in Fibrous Materials: the use of Planck Mean Properties compared to Spectral and Flux-weighted Properties.

F.M.B. Andersen
Department of Energy Engineering
Technical University of Denmark
2800 Lyngby, Denmark.

S. Dyrbøl
Rockwool International A/S and
Department of Buildings and Energy
Technical University of Denmark.
2800 Lyngby, Denmark.

ABSTRACT

Radiative heat transport was investigated in a layer of fibrous insulation under steady-state conditions. It was modelled using the two-flux model, where the radiative properties are either Planck mean, flux-weighted or spectral properties. The purpose of the work was to investigate the accuracy of the radiative flux obtained using Planck mean properties, by comparing with spectral calculations. This was achieved by deriving and investigating a mathematical basis for applying Planck mean properties in the two-flux model and by comparing Planck mean properties to flux-weighted properties, defined in such a way that the same solution was obtained as in the spectral calculations.

The mathematical assumptions justifying the application of Planck mean properties were correct within ±1% for wavelengths greater than approx. 10 μm. For wavelengths ranging from 1 to 10 μm, the deviation was up to 60%. Using Planck mean properties, the radiative heat flux in the centre of the fibrous insulation was underpredicted by about 15% for porosities lower than approx. 0.995 and by less for higher porosities. The solution of radiative heat flux depends to a large extent on the asymmetry in the flux-weighted properties. For example, if the flux-weighted properties are asymmetric within one percent, then the radiative heat flux increases by a factor of 5 and 14 in cases with a porosity of 0.98 and 0.9937, respectively. The asymmetry in the flux-weighted properties may explain why the small deviation from the mathematical assumption leading to the Planck mean gives large errors.

INTRODUCTION

Fibrous insulation is widely used for the thermal insulation of machinery and buildings, to conserve energy and to create acceptable conditions for humans. Due to its widespread use and economic significance, it is important to be able to model the different types of heat transfer that occur in fibrous insulation in order to improve the performance or economy of the material. Since radiative heat transfer accounts for about thirty percent or more of the total heat transport at room temperature, radiative heat transfer cannot be disregarded.

The analysis concerns a layer of fibrous insulation placed between two walls heated to 293.15 K and cooled to 273.15 K, respectively (Fig. 1).

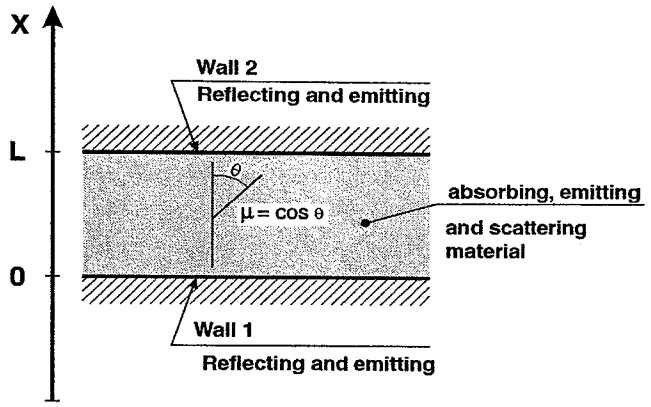

Figure 1: Geometry of the fibrous insulation.

Several authors have discussed the applicability of mean radiative properties. Viskanta[1] investigated radiation in an absorbing-emitting gas and obtained integral equations for mean absorption coefficients and for mean emission coefficients; he emphasized that the mean radiative properties can first be obtained when the spectral solution is known. Traugott[2] used a multi-equation-moment model for studying gas radiation and showed that the absorption coefficient must be defined differently in the various moment equations. Patch[3] suggested a possible weighting scheme for calculating the mean radiative properties for gas and obtained results that were within 28% of the spectral solution, while using the Planck mean properties yielded errors as high as 455%. In optically thick media, the radiative diffusion equation can be applied using the Rosseland mean properties (Caps et al.[4]). The limitations of the diffusion models are several but well described in Siegel and Howell[5]. However, the Planck mean properties are often applied (e.g. by Tong et al.[6]), mainly due to the simplicity of the weighting process and the lack of better alternatives. Viskanta and Mengüc[7] reviewed the literature dealing with mean weighted radiative properties and give further references.

The results obtained from radiative analyses of gas, e.g. concerning the accuracy of using the Planck mean properties, cannot be assumed to be valid also for fibrous insulation since the spectral properties of gases vary much more with the wavelength than do those of a dispersed medium of fibres. Neither can results from radiative analyses of pulverized coal-fired furnaces be transferred to the actual cases due to differences in temperature level, particle shape, porosity and complex refractive index. There appears to be a lack of knowledge concerning the accuracy of using the Planck mean properties for modelling fibrous insulation material.

The advantage of using mean radiative properties in the two-flux model is that the radiative heat fluxes are modelled by no more than two differential equations, while spectral analysis requires the solution of a number of differential equations (twice the number of wavelength bands). Using mean radiative properties simplifies the problem and reduces computation time as there are fewer differential equations, but it may introduce errors.

The main purpose of this work is to investigate the accuracy of the radiative heat flux obtained using the Planck mean properties in the two-flux radiative model, compared to the detailed spectral two-flux model, in the case of fibrous insulation. The accuracy is investigated by using flux-weighted properties, defined in such a way that the same solution is obtained as in the spectral calculations.

METHOD

In order to derive the equations for heat transport by conduction and radiation, the following assumptions were made:

- a steady-state condition;
- one-dimensional heat conduction;
- the gas inside the fibrous insulation is stagnant dry air at atmospheric pressure;
- the walls enclosing the insulation are perfect diffuse emitters and reflectors and are isothermal;
- the intensity in the forward and backward hemispheres is constant;
- the radiative properties of the fibrous insulation and the walls are constants in a wavelength band.

The above assumptions leads to a system of ordinary differential equations from which the temperature and radiation can be determined.

Energy Conservation Equation

The steady-state energy equation for the gas and fibre in the insulation was:

$$\frac{d}{dx}\left(-\lambda_{eff}\frac{dT}{dx}\right)+\frac{dq^r}{dx}=0 \tag{1}$$

where the temperature of fibres and gas are assumed to be equal.

Two-Flux Radiation Model

The spectral two-flux model (STF) (Siegel and Howell[5], Tong and Tien[8], Brewster[9]) is:

$$\frac{dq_\lambda^+}{dx}=-2\cdot(\sigma_{a\lambda}+b_\lambda\cdot\sigma_{s\lambda})\cdot q_\lambda^+ +2\cdot\sigma_{a\lambda}\cdot e_{b\lambda}+2\cdot b_\lambda\cdot\sigma_{s\lambda}\cdot q_\lambda^- \tag{2}$$

$$-\frac{dq_\lambda^-}{dx}=-2\cdot(\sigma_{a\lambda}+b_\lambda\cdot\sigma_{s\lambda})\cdot q_\lambda^- +2\cdot\sigma_{a\lambda}\cdot e_{b\lambda}+2\cdot b_\lambda\cdot\sigma_{s\lambda}\cdot q_\lambda^+ \tag{3}$$

The divergence of the total radiative heat flux applied in eq. (1) was obtained by adding eqs. (2) and (3) and integrating over the wavelength spectrum.

$$\frac{dq^r}{dx}=4\int_0^\infty \sigma_{a\lambda}\cdot e_{b\lambda}\cdot d\lambda-2\int_0^\infty \sigma_{a\lambda}\cdot(q_\lambda^+ +q_\lambda^-)\cdot d\lambda \tag{4}$$

The Boundary Conditions

The conditions were:

$$T(0)=T_{w1} \qquad T(L)=T_{w2} \tag{5,6}$$

$$q_\lambda^+(0)=\rho_{w1\lambda}\cdot q_\lambda^-(0)+\varepsilon_{w1\lambda}\cdot e_{b\lambda}(T_{w1}) \tag{7}$$

$$q_\lambda^-(L)=\rho_{w2\lambda}\cdot q_\lambda^+(L)+\varepsilon_{w2\lambda}\cdot e_{b\lambda}(T_{w2}) \tag{8}$$

Iterative Numerical Solution Technique

The divergence of the radiative heat flux was estimated to be linear at first in all the grid points. These values were used in the finite difference discretized energy equation, and the temperature distribution was obtained using a tri-diagonal solver. The temperature distribution was used to obtain the q^+_λ and q^-_λ in all the wavelength bands, from the finite difference discretized two-flux equations using a tri-diagonal block solver where the blocks were 2×2 matrices. Updated values of dq^r/dx were calculated from eq. (4) using q^+_λ and q^-_λ, and the temperatures. The discretized energy equation was solved again using the updated dq^r/dx. The updated temperatures were then used to solve the radiation equation. The iteration continued until convergence. To speed up convergence, underrelaxation factors were applied for the temperature and for dq^r/dx. An optimal value of 0.88 for the underrelaxation factor for both the temperature and dq^r/dx was obtained when the porosity was 0.9937. The computer code uses an equidistant grid, and the number of grid points used in this investigation to give grid-independent solutions was found to be 500.

Mean Radiative Coefficients

Equations for the radiative heat flux in the forward and backward hemispheres can be found by integrating the spectral two-flux model over the total wavelength domain:

$$\frac{dq^+}{dx} = -2\int_{\lambda=0}^{\infty}(\sigma_{a\lambda}+b_\lambda\cdot\sigma_{s\lambda})\cdot q^+_\lambda\cdot d\lambda + 2\int_{\lambda=0}^{\infty}\sigma_{a\lambda}\cdot e_{b\lambda}\cdot d\lambda + 2\int_{\lambda=0}^{\infty} b_\lambda\cdot\sigma_{s\lambda}\cdot q^-_\lambda\cdot d\lambda \tag{9}$$

$$-\frac{dq^-}{dx} = -2\int_{\lambda=0}^{\infty}(\sigma_{a\lambda}+b_\lambda\cdot\sigma_{s\lambda})\cdot q^-_\lambda\cdot d\lambda + 2\int_{\lambda=0}^{\infty}\sigma_{a\lambda}\cdot e_{b\lambda}\cdot d\lambda + 2\int_{\lambda=0}^{\infty} b_\lambda\cdot\sigma_{s\lambda}\cdot q^+_\lambda\cdot d\lambda \tag{10}$$

Introducing the flux-weighted properties and the Planck mean properties defined as follows:

$$\overline{\sigma_a}^+ = \frac{1}{q^+}\int_{\lambda=0}^{\infty}\sigma_{a\lambda}\cdot q^+_\lambda\cdot d\lambda \qquad \overline{\sigma_a}^- = \frac{1}{q^-}\int_{\lambda=0}^{\infty}\sigma_{a\lambda}\cdot q^-_\lambda\cdot d\lambda \tag{11,12}$$

$$\overline{\sigma_a}_{Pl} = \frac{1}{e_b}\int_{\lambda=0}^{\infty}\sigma_{a\lambda}\cdot e_{b\lambda}\cdot d\lambda \tag{13}$$

$$\overline{b\sigma_s}^- = \frac{1}{q^-}\int_{\lambda=0}^{\infty} b_\lambda\cdot\sigma_{s\lambda}\cdot q^-_\lambda\cdot d\lambda \qquad \overline{b\sigma_s}^+ = \frac{1}{q^+}\int_{\lambda=0}^{\infty} b_\lambda\cdot\sigma_{s\lambda}\cdot q^+_\lambda\cdot d\lambda \tag{14,15}$$

yielded the two-flux model with flux-weighted radiative properties (FWTF):

$$\frac{dq^+}{dx} = -2(\overline{\sigma_a}^+ + \overline{b\cdot\sigma_s}^+)\cdot q^+ + 2\overline{\sigma_a}_{Pl}\cdot e_b + 2(\overline{b\cdot\sigma_s}^-)\cdot q^- \tag{16}$$

$$-\frac{dq^-}{dx} = -2(\overline{\sigma_a}^- + \overline{b\cdot\sigma_s}^-)\cdot q^- + 2\overline{\sigma_a}_{Pl}\cdot e_b + 2(\overline{b\cdot\sigma_s}^+)\cdot q^+ \tag{17}$$

and the divergence

$$\frac{dq^r}{dx} = 4\cdot\overline{\sigma_a}_{Pl}\cdot e_b - 2\cdot(\overline{\sigma_a}^+\cdot q^+ + \overline{\sigma_a}^-\cdot q^-) \tag{18}$$

It will be noted that the flux-weighted radiative properties as defined in eqs. (11, 12) and (14, 15), depend not only on the spectral properties ($\sigma_{a\lambda}$, $\sigma_{s\lambda}$, b_λ), but also on the relative spectral radiative fluxes q^+_λ/q^+ and q^-_λ/q^-. Thus it is not possible to calculate the flux-weighted radiative properties without knowing the spectral solution for q^+_λ and q^-_λ.

Assuming that $e_{b\lambda}/e_b = q^+_\lambda/q^+ = q^-_\lambda/q^-$, the flux-weighted radiative properties in eqs. (11, 12) and (14, 15) become the Planck mean properties:

$$\overline{\sigma_a}^+ = \overline{\sigma_a}^- = \overline{\sigma_a}_{Pl} \tag{19}$$

$$\overline{b\sigma_s}^+ = \overline{b\sigma_s}^- = \overline{(b\sigma_s)}_{Pl} = \frac{1}{e_b}\int_{\lambda=0}^{\infty} b_\lambda \cdot \sigma_{s\lambda} \cdot e_{b\lambda} \cdot d\lambda \tag{20}$$

and the two-flux equation with the Planck mean properties (Planck-TF) becomes:

$$\frac{dq^+}{dx} = -2 \cdot (\overline{\sigma_a}_{Pl} + \overline{(b \cdot \sigma_s)}_{Pl}) \cdot q^+ + 2 \cdot \overline{\sigma_a}_{Pl} \cdot e_b + 2\overline{(b \cdot \sigma_s)}_{Pl} \cdot q^- \tag{21}$$

$$-\frac{dq^-}{dx} = -2 \cdot (\overline{\sigma_a}_{Pl} + \overline{(b \cdot \sigma_s)}_{Pl}) \cdot q^- + 2 \cdot \overline{\sigma_a}_{Pl} \cdot e_b + 2 \cdot \overline{(b \cdot \sigma_s)}_{Pl} \cdot q^+ \tag{22}$$

and the divergence

$$\frac{dq^r}{dx} = 4 \cdot \overline{\sigma_a}_{Pl} \cdot e_b - 2 \cdot \overline{\sigma_a}_{Pl} \cdot (q^+ + q^-) \tag{23}$$

NUMERICAL RESULTS AND DISCUSSION

The absorption and scattering efficiencies were calculated using the computer code of Tong and Gritzo[10], which is valid for infinitely long circular cylindrical fibres with a constant complex refraction index throughout the fibre, i.e. fibres that are not coated or stratified. The complex refractive index from Hsieh and Su[11] was used for 1.0 μm<λ<206.6 μm, and for λ>206.6 μm the index was assumed to be constant and equal to the values at λ=206.6 μm. The absorption and scattering properties are then calculated for 48 wavelength bands, taking into account the diameter distribution and the porosity and assuming that the fibres are all randomly oriented parallel to the walls, using the appropriate equations given by Tong et al.[6] and Dombrovsky[12].

The diameter distribution shown in Fig. 2 was used in calculating the radiative properties. The spectral absorption and scattering coefficients calculated from the efficiencies, which have been divided into 48 wavelength bands, are shown in Fig. 3.

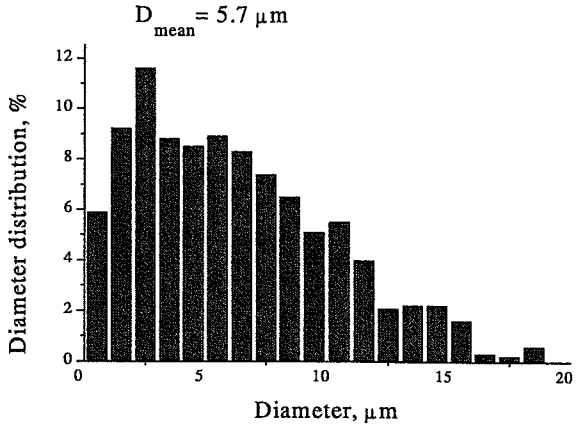

Figure 2:
Diameter distribution.

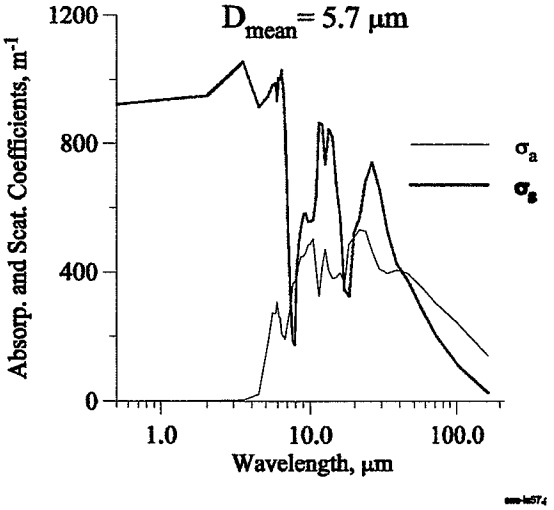

Figure 3:
Spectral radiative properties at temperature 283.15K and with a porosity of 0.9973.

The two-flux model in eqs. (21) and (22) using the Planck mean radiative properties was derived assuming that $e_{b\lambda}/e_b = q^+_\lambda/q^+ = q^-_\lambda/q^-$. If this assumption is not correct, the radiation solution using the Planck mean properties will not be exact. In order to investigate the errors introduced by the assumption , the relative ratios:

$$\frac{\frac{q^+_\lambda}{e_{b\lambda}}}{\frac{q^+}{e_b}} \quad \text{and} \quad \frac{\frac{q^-_\lambda}{e_{b\lambda}}}{\frac{q^-}{e_b}} \qquad (24,25)$$

calculated from the spectral solution are shown in Figs. 4 and 5 for several porosities.

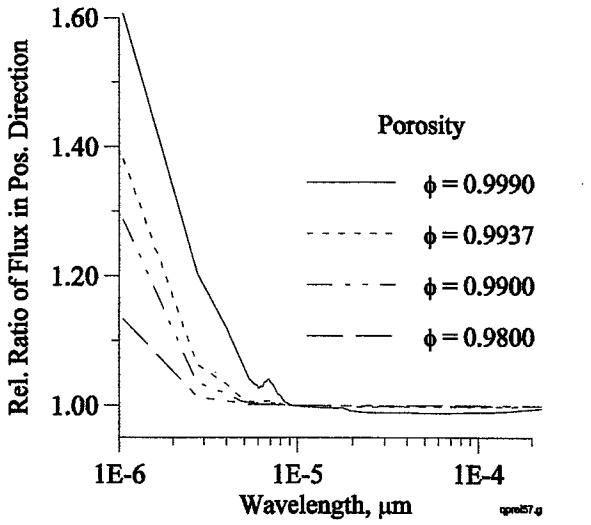

Figure 4:
Ratios of q^+_λ/q^+ to $e_{b\lambda}/e_b$ as function of wavelength by several porosities.

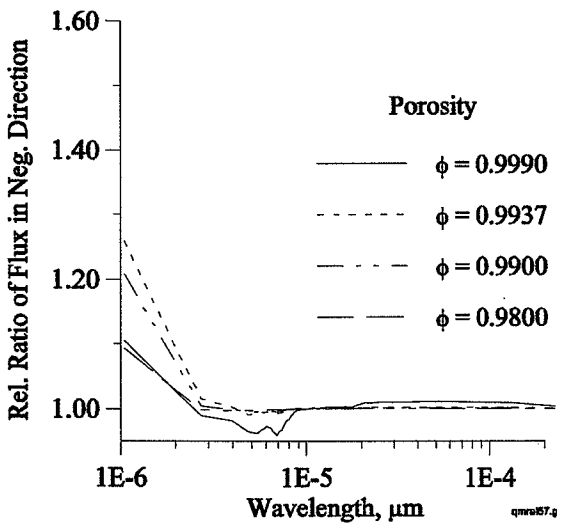

Figure 5:
Ratios of q^-_λ/q^- to $e_{b\lambda}/e_b$ as function of wavelength by several porosities.

If the assumption $e_{b\lambda}/e_b = q^+_\lambda/q^+ = q^-_\lambda/q^-$ is correct, the ratios in (24) and (25) will be unity. Figures 4 and 5 show that the deviation from unity depends on the porosities and the wavelength. However, it should be remembered that ninety percent of the energy emitted from a blackbody at temperature 283.15 K is in the wavelength range 6.65 μm to 44.0 μm, with a maximum at 10.2 μm. The mathematical assumption justifying the application of Planck mean properties was correct within ±1% for wavelengths higher than 10 μm in the cases investigated. For wavelengths from 1 to 10 μm, the deviation from unity was up to 60%. The deviation from unity is notable only at very few wavelengths in the high energy range and only for a porosity of 0.9990. At very high porosities, the use of Planck mean properties is not expected to cause any notable error in the calculation of the radiative heat transfer, since the radiative properties will approach zero.

The flux-weighted mean radiative properties $\overline{\sigma_a}^+, \overline{\sigma_a}^-, \overline{b\sigma_s}^+$ *and* $\overline{b\sigma_s}^-$ have been calculated using eqs. (11,12) and (14,15) and the spectral solution was obtained using 48 wavelength bands. The integrals of eqs. (11,12) and (14,15) were easily obtained by summation since the radiation properties are considered as constants within each wavelength band and the radiation fluxes in each band are integral values for the band. To illustrate the calculations, $\overline{\sigma_a}^+$ was obtained using eq. (11) as follows:

$$\overline{\sigma_a}^+ = \frac{1}{q^+}\int_0^\infty \sigma_{a\lambda} q^+_\lambda d\lambda = \frac{1}{q^+}\sum_{j=1}^{Nband} \sigma_{aj} \int_{\lambda_j}^{\lambda_{j+1}} q^+_\lambda d\lambda = \frac{1}{q^+}\sum_{j=1}^{Nband} \sigma_{aj} q^+_j \qquad (26)$$

and the other flux-weighted radiative properties were obtained similarly. The flux-weighted properties and the Planck mean properties are given in Table 1.

ϕ	$\overline{\sigma_a}^+$ [m^{-1}]	$\overline{\sigma_a}^-$ [m^{-1}]	$\overline{b\sigma_s}^+$ [m^{-1}]	$\overline{b\sigma_s}^-$ [m^{-1}]	$\overline{\sigma_a}_{Pl}$ [m^{-1}]	$\overline{b\sigma_s}_{Pl}$ [m^{-1}]
0.9800	1316.00	1316.30	240.582	240.663	1315.83	240.565
0.9900	657.850	658.200	120.266	120.347	657.896	120.276
0.99373	412.330	412.670	75.3805	75.4606	412.439	75.4000
0.99700	197.190	197.530	36.0491	36.1289	197.352	36.0772
0.99800	131.400	131.720	24.0189	24.0983	131.563	24.0499
0.99900	65.6180	65.9160	11.9902	12.0672	65.7784	12.0239
0.99950	32.7590	33.0010	5.98037	6.04806	32.8883	6.01163
0.99990	6.53830	6.61270	1.19048	1.21540	6.57779	1.20237
0.99995	3.26880	3.30670	0.59493	0.60800	3.28903	0.60123

Table 1:
Flux-weighted and Planck mean radiative properties.

In order to investigate the application of the Planck mean properties, the flux-weighted properties were made dimensionless using the Planck mean properties as follows:

$$\frac{\overline{\sigma_a}^+}{\overline{\sigma_a}_{Pl}}, \frac{\overline{\sigma_a}^-}{\overline{\sigma_a}_{Pl}}, \frac{\overline{b\sigma_s}^+}{\overline{b\sigma_s}_{Pl}} \text{ and } \frac{\overline{b\sigma_s}^-}{\overline{b\sigma_s}_{Pl}} \qquad (27\text{-}30)$$

In the cases where the Planck mean properties gave an exact solution, the ratios were unity. The dimensionless properties in eqs. (27-30) are shown in Fig. 6, calculated from the spectral solution. It will be seen that the deviation from unity is an increasing function of the porosity. These deviations are relative and the absolute deviations are decreasing functions of the porosity, as shown in Fig. 7.

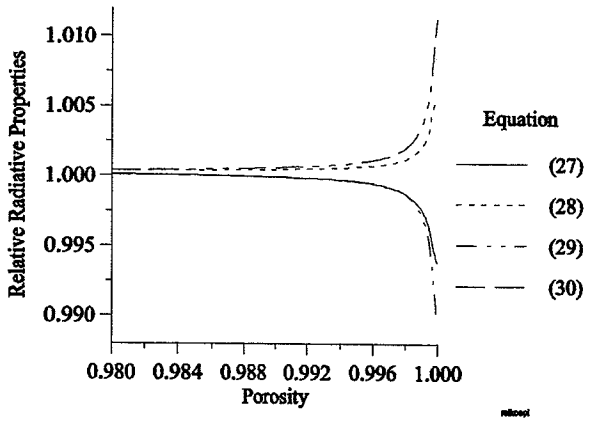

Figur 6:
Ratios of flux-weighted properties to Planck mean properties using eqs. (11) to (15) and (20).

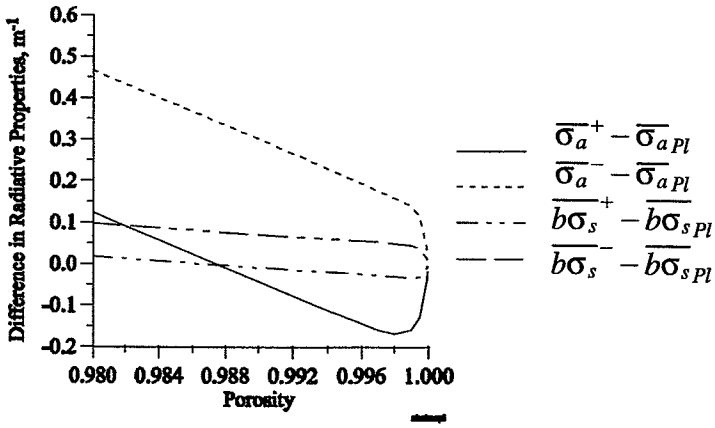

Figur 7:
Difference between flux-weighted properties and Planck mean properties.

Figure 6 shows that the negative flux-weighted radiative properties, i.e. $\overline{\sigma_a}^-$ and $\overline{b\sigma_s}^-$, were generally higher than the Planck mean properties and the positive flux-weighted properties, i.e. $\overline{\sigma_a}^+$ and $\overline{b\sigma_s}^+$, were lower than the Planck mean properties. This fact creates an asymmetry in the FWTF (eqs. (16) and (17)) which exists neither in the STF (eqs. (2) and (3)) nor in the Planck-TF (eqs. (21) and (22)).

Figure 8 shows the radiative heat flux calculated using the STF, the FWTF and the Planck-TF in the centre grid point. The FWTF is a mathematical consequence of the STF which means that the use of flux-weighted properties always gives exactly the same results as the STF. This is confirmed by Figs. 8 and 9. The drawback of the FWTF is that the flux-weighted properties must be obtained from integrations using the spectral fluxes and these fluxes are not known. This disadvantage makes the practical use of flux-weighted properties useless in most cases. However, the analysis leading to the FWTF, as well as the numerical calculations of the flux-weighted properties show that there is an asymmetry in the radiative properties as well as in the FWTF. It is anticipated that the asymmetry in the flux-weighted properties can explain why the small deviation from the mathematical assumption leading to the Planck mean gives large errors.

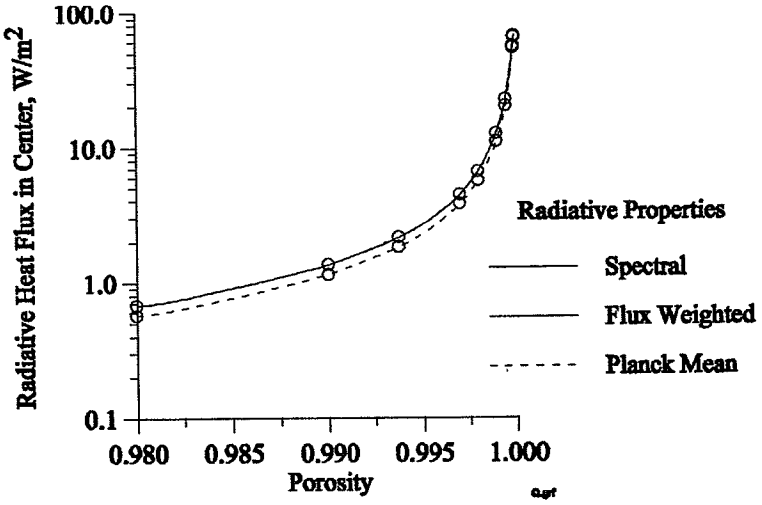

Figure 8:
Radiative heat flux in the centre grid point as a function of porosity.

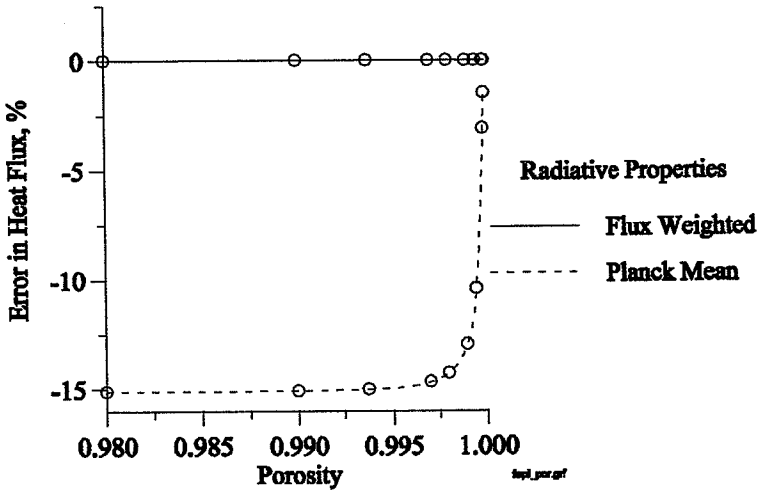

Figure 9:
Errors in heat flux obtained by flux-weighted properties and Planck mean properties.

The errors in the radiative heat flux when using the FWTF and the Planck-TF are shown in Fig. 9. Using flux-weighted properties evaluated at the centre point gave a maximum error of less than 0.02% compared to spectral calculations. The deviation is presumably caused by having used the flux-weighted properties of the centre grid point in all the grid points. Instead, the flux-weighted properties should be calculated in all grid points from the spectral solution. Using Planck mean properties underpredicted the radiative heat flux by about 15% for porosities lower thanapprox. 0.995. When the porosity approaches unity, the error approaches zero. This can be explained as follows: when the porosity approaches unity, the radiative properties of the fibrous material approach zero and the material is non-absorbing and non-scattering. The radiative heat flux then depends only on the temperature and the radiative properties of the walls, and may be calculated from the well known equations for radiative heat exchange between two infinite parallel plates with a transparent medium between. Other weighting procedures of the radiative properties should show similar results as the porosity approaches unity.

To investigate further the influence of asymmetric radiative properties, these have been varied systematically around the Planck mean properties in Table 2, so that the positive flux-weighted properties, $\overline{\sigma_a}^+$ and $\overline{b\sigma_s}^+$, were lower than the Planck mean properties and the negative flux-weighted properties were similarly higher than the Planck mean values. The properties were applied in eqs. (16) and (17) and the resulting radiative heat flux in the centre grid point was compared to the radiative heat flux obtained when using Planck mean properties. For a porosity of 0.9800, the results in Table 2 show that when the absorption coefficients $\overline{\sigma_a}^+$ and $\overline{\sigma_a}^-$ were each decreased and increased by 1%, the predicted radiative heat flux increased by a factor of 10.37. When a similar decrease and increase in the values $\overline{b\sigma_s}^+$ and $\overline{b\sigma_s}^-$ occurred the radiative heat flux changed by a factor of 4.41. When the values changed ±2%, the increase was approximately twice as great. When the properties $\overline{\sigma_a}^+$ and $\overline{b\sigma_s}^+$ were both decreased and $\overline{\sigma_a}^-$ and $\overline{b\sigma_s}^-$ were both increased, the predicted radiative heat flux increased by a factor of 13.82. The calculation of the radiative heat flux was found to be very sensitive to asymmetry in the radiative properties. Consequently, the flux-weighted properties may explain why the small deviation from the mathematical assumption leading to the Planck mean results in large errors. If the properties were made asymmetric within one percent, then the radiative heat flux would increase by a factor of 5 and 14 in the cases presented in Table 2.

$\overline{\sigma_a}^+$ [m^{-1}]	$\overline{\sigma_a}^-$ [m^{-1}]	$\overline{b\sigma_s}^+$ [m^{-1}]	$\overline{b\sigma_s}^-$ [m^{-1}]	$\frac{\bar{q}_{FW}}{\bar{q}_{Pl}}$ ϕ=0.9800	$\frac{\bar{q}_{FW}}{\bar{q}_{Pl}}$ ϕ=0.99373
$1.00 \cdot \overline{\sigma_{a\,Pl}}$	$1.00 \cdot \overline{\sigma_{a\,Pl}}$	$1.00 \cdot \overline{b\sigma_{s\,Pl}}$	$1.00 \cdot \overline{b\sigma_{s\,Pl}}$	1.00	1.00
$0.99 \cdot \sigma_{aPl}$	$1.01 \cdot \overline{\sigma_{a\,Pl}}$	$1.00 \cdot \overline{b\sigma_{s\,Pl}}$	$1.00 \cdot \overline{b\sigma_{s\,Pl}}$	10.37	3.94
$0.98 \cdot \overline{\sigma_{a\,Pl}}$	$1.02 \cdot \overline{\sigma_{a\,Pl}}$	$1.00 \cdot \overline{b\sigma_{s\,Pl}}$	$1.00 \cdot \overline{b\sigma_{s\,Pl}}$	19.84	6.90
$1.00 \cdot \overline{\sigma_{a\,Pl}}$	$1.00 \cdot \overline{\sigma_{a\,Pl}}$	$0.99 \cdot \overline{b\sigma_{s\,Pl}}$	$1.01 \cdot \overline{b\sigma_{s\,Pl}}$	4.41	2.07
$1.00 \cdot \overline{\sigma_{a\,Pl}}$	$1.00 \cdot \overline{\sigma_{a\,Pl}}$	$0.98 \cdot \overline{b\sigma_{s\,Pl}}$	$1.02 \cdot \overline{b\sigma_{s\,Pl}}$	7.84	3.15
$0.99 \cdot \overline{\sigma_{a\,Pl}}$	$1.01 \cdot \overline{\sigma_{a\,Pl}}$	$0.99 \cdot \overline{b\sigma_{s\,Pl}}$	$1.01 \cdot \overline{b\sigma_{s\,Pl}}$	13.82	5.02

Table 2:
Influence of the asymmetry in the radiative properties. The absolute value of the radiative properties is given i Table 1 and the radiative flux calculated by the use of Planck mean properties is $q_{Pl\,(x=0.05m)}$=0.5731 W/m^2 at ϕ=0.9800 and $q_{Pl\,(x=0.05m)}$=1.8265 W/m^2 at ϕ=0.99373.

CONCLUSION

The investigation has led to the following conclusions:

- The mathematical assumption justifying the application of Planck mean properties is correct within ±1% for wavelengths greater than 10 μm. For wavelengths ranging from 1 to 10 μm, the deviation is up to 60% in the cases investigated.

- Using Planck mean properties underpredicts the radiative heat flux in the centre of the fibrous insulation by about 15% for porosities lower than approx. 0.995 and less for higher porosities.

- The solution of the radiative heat flux is very sensitive to the asymmetry in the flux-weighted properties.

NOMENCLATURE

Latin letters

b	backscatter factor
D	fibre diameter [m]
e_b	blackbody emissive power [W/m^2], total or [W/m^3], spectral
L	thickness of the insulation layer [m]
q	heat flux [W/m^2]
T	temperature [K]
x	location [m]

Greek letters

ε	emissivity of wall
ϕ	porosity
λ	thermal conductivity [W/m/K]
ρ	reflectivity of wall
σ_a	absorption coefficient [m^{-1}]
σ_s	scattering coefficient [m^{-1}]

Subscript/superscript

eff	effective property
FW	Flux-weighted
j	integer
Pl	Planck mean
r	radiation
w1	wall 1
w2	wall 2
λ	wavelength
+/-	positive/negative direction

Abbreviation

FWTF	two-flux model with flux-weighted properties
Nband	number of wavelength band
Planck-TF	two-flux model with Planck mean properties
STF	two-flux model with spectral radiative properties

REFERENCES

1. Viskanta R., "Concerning the definitions of the mean absorption coefficient", *International Journal of Heat and Mass Transfer*, Vol. 7, pp.1047-1049, 1964.
2. Traugott S.C., "On grey absorption coefficients in radiative transfer" *J.Quant. Spectrosc. Radiat. Transfer,* Vol. 8, pp 971-999, 1968.
3. Patch R.W., "Effective absorption coefficients for radiant energy transport in nongrey, nonscattering gases", *J.Quant. Spectrosc. Radiat. Transfer,* Vol. 7, pp. 611-637, 1967.
4. Caps R., Arduini-Schuster M.C., Ebert H.P., Fricke J.,"*Improved thermal radiation extinction in metal coated polypropylen microfibers*", Physikalisches Institut der Universität Würzburg, Germany, Report E21-0392-2, 1992.
5. Siegel R. and Howell J.R., "*Thermal Radiation Heat Transfer*", Hemisphere Publishing Corporation, 3rd. ed., 1992.
6. Tong T.W., Sathe S.B. and Peck R.E., "Improving the Performance of Porous Radiant Burners through use of Sub-micron size Fibers", *Int. J. Heat Mass Transfer*, Vol. 33, No. 6, pp.1339-1346, 1990.
7. Viskanta R., Mengüc M." Radiation heat transfer in combustion systems", *Prog. Energy Combust. Sci.* Vol.13, pp.97-160, 1987.
8. Tong T.W.and Tien C.L., "Analytical Models for Thermal Radiation in Fibrous Insulations", *Journal of Thermal Insulation*, Vol.4, pp.27-44, 1980.
9. Brewster M.Q.,"*Thermal Radiative Transfer & Properties*", John Wiley and Sons, Inc. New York, 1992.
10. Tong T.W. and Gritzo L.A.,"*Mathematical Modeling of Scattering of Radiation in Radiative Heat Transfer*", Sandia National Laboratories, Thermal and Fluid Engineering, Dept. 1513, Albuquerque, Development Project 7159.051, 1993.
11. Hsieh C.K., and Su K.C., "Thermal Radiative Properties of Glass from 0.32 to 206 μm", *Solar Energy*, Vol. 22, pp. 37-43, 1979.
12. Dombrovsky L.A., "Quartz-Fiber Thermal Insulation: Infrared Radiative Properties and Calculation of Radiative-Conductive Heat Transfer", *Journal of Heat Transfer,* Vol. 118, pp.408-414, 1996.

Appendix C

Orientation estimation

The Fourier spectrum is approximated by an ellipse fitted to the power spectrum centred at (0, 0). In order to eliminate "noise" in the image the magnitude of the Fourier spectrum (the pixel values) have been raise to the fourth power which means that low signals in the Fourier spectrum will not affect the result.

The dispersion matrix is assumed to be positive definite, and is given by eq. (c.1):

$$\Pi = \begin{pmatrix} \sigma_x^2 & \sigma_{xy} \\ \sigma_{xy} & \sigma_y^2 \end{pmatrix} \tag{c.1}$$

in which

$$\sigma_x^2 = \sum_x \sum_y x^2 p(x, y) \tag{c.2}$$

$$\sigma_y^2 = \sum_x \sum_y y^2 p(x, y) \tag{c.3}$$

$$\sigma_{xy} = \sum_x \sum_y x \cdot y \cdot p(x, y) \tag{c.4}$$

(x, y) is the distance from the centre in the Fourier domain and p(x,y) is the normalised (estimated) power spectrum:

$$p(x, y) = \frac{P(x, y)}{\sum_{(x,y)\neq(0,0)} P(x, y)} \tag{c.5}$$

in which P(x,y) is the magnitude of the Fourier spectrum raised in the fourth power. The eigenvalues to the positive definite symmetrical matrix in eq. (c.1) are:

$$\lambda_1 = \frac{(\sigma_x^2 + \sigma_y^2 + \sqrt{(\sigma_x^2 - \sigma_y^2)^2 + 4\sigma_{xy}^2})}{2} \tag{c.6}$$

$$\lambda_2 = \frac{(\sigma_x^2 + \sigma_y^2 - \sqrt{(\sigma_x^2 - \sigma_y^2)^2 + 4\sigma_{xy}^2})}{2} \tag{c.7}$$

The corresponding normalised eigenvectors become:

$$P_i = \left(\frac{\sigma_{xy}}{\sqrt{\sigma_{xy}^2 + (\lambda_i - \sigma_x^2)^2}}; \frac{\lambda_i - \sigma_x^2}{\sqrt{\sigma_{xy}^2 + (\lambda_i - \sigma_x^2)^2}} \right) \quad i = 1,2 \qquad \text{(c.8)}$$

In a perfectly orientated image the ellipse fitted to the power spectrum will have one of the eigenvalues which will be zero, as opposed to a perfectly homogeneous image, where the eigenvalues will be equal.

The direction of the larger eigenvector (the major axis in the ellipse) can then be used as an estimate of the dominant direction in the analysed local texture and the difference between the larger and the smaller eigenvalue as a measure of the consistency in the orientation.

List of correction:

Heat transfer in Rockwool Modelling and method of measurement

Part II: Modelling radiative heat transfer in fibrous materials

Page	paragraph/line	Correction (underlined is changed or added)
17	3rd paragraph, 1st line	computer code
18	1st paragraph, 4th line	eq. (~~3.6~~) (4.1)
19	2nd paragraph, 2nd line	figure ~~3.~~ 4.2
	2nd line from bottom	Figure ~~3.~~ 4.3
20	1st paragraph, 5th line	figure ~~3.~~ 4.3.
21	2nd paragraph, 2nd line	eq. (~~3.11~~) (4.2)
	3rd paragraph, 2nd line	(π/2-α, figure ~~3.3~~) (π/2-α, figure 4.2)
	7th line from bottom	figure ~~3.3~~ 4.4
22	1st line	eq. (~~3.2~~) and () (4.3) and (4.4)
	3rd line from top	eq. () (4.4)
	6th line from top	eq. (~~3.2~~) (4.3)
	7th line from top	eq. (~~3.3~~) (4.5)
	9th line from top	figure ~~3.2~~ figure 4.4 … eq. (~~3.2 3.3~~) (4.3 – 4.5)
	18th line from top	eq. (~~3.10~~) eqs. (4.6 – 4.7)